本文已被《SIAM优化杂志》接受发表。
This paper has been accepted for publication in SIAM Journal on Optimization.

SET-MEMBERSHIP LOCALIZATION VIA RANGE MEASUREMENTS

GIUSEPPE C. CALAFIORE*

Abstract. In this paper we discuss classical geometrical problems of estimating an unknown point location from several noisy measurements of the Euclidean distances from that point to a set of known reference points (anchors). We approach the problem via a set-membership methodology, in which we assume the distance measurements to be affected by unknown-but-bounded errors, and we characterize the set of all points that are consistent with the measurements and their assumed error model. This set is nonconvex, but we show in the paper that it is contained in a region given by the intersection of certain closed balls and a polytope, which we call the *localization set*. Then, we develop efficient methods, based on convex programming, for computing a tight outer-bounding set of simple structure (a box, or an ellipsoid) for the localization set, which then acts as a guaranteed set-valued location estimate. The center of the bounding set also serves as a point location estimate. Related problems of inner approximation of the localization set via balls and ellipsoids are also posed as convex programming problems. Different from existing methods based on semidefinite programming relaxations of a nonconvex cost minimization problem, our approach is direct, geometric and based on a polyhedral set of points that satisfy pairwise differences of the measurement equations.

Key words. multilateration, GPS, range measurements, interval calculus, set-membership estimation, convex optimization.

MSC codes. 65G40, 62F30, 68U99, 52A27, 52B55, 62G15, 65D99, 90C25, 90C90

1. Introduction.

Estimating the location of a point in space from several measurements of its distances from known reference points is a basic problem in many applications, including wireless sensor networks, robotics and navigation, machine learning, and more. Typical applications include the localization of a vessel, aircraft, robot, etc., based on range (distance) measurements from multiple known reference points, called beacons or anchors. Depending on the application, the distance measurements can be inferred from the time of arrival (TOA) or time difference of arrival (TDoA) of signals from beacons, from direct laser measurements, from received signal strength, etc.

The problem is classical, and a huge literature on the subject has been developed since the 1980s and early 1990s; see, e.g., [2, 4] and the references therein for some classical results dating back to the 1980s, and [1, 3, 5, 6, 7, 8, 9, 10, 11, 12, 13, 14, 15, 16, 17, 18, 19, 20, 21, 22, 23, 24, 25, 26] for more recent results. We refer the reader also to the recent review paper [27] for a complete survey of the topic of multilateration, its applications, and pointers to relevant references. In the typical approach to multilateration, an objective criterion is constructed which accounts for the sum of residuals between measurements and point-to-beacon distances, and such objective is then minimized with respect to the unknown position by means of optimization techniques. The main issue in this respect is that the objective takes typically the form of a nonlinear Least Squares problem, hard to manage and solve. Maximum Likelihood estimation problems, in fact, usually take the form of nonlinear Least Squares problems. Even when the measurement errors are assumed to be Gaussian, the resulting Maximum Likelihood estimation problem is typically nonconvex, and difficult to solve globally. Certain approaches, see e.g., [4], hence apply convex relaxation techniques to obtain an approximate problem that is amenable to solution via semidefinite programming solvers. A different approach, called the *squared-range-based least squares* (SR-LS), applies instead a Least Squares methodology to the *squared* distance measurements, see again [4]. This also results in a nonconvex problem formulation, which is amenable to approximate solution via relaxation. Along this line of minimizing a sum of measurement equation errors via convex relaxation, in the more general context of sensor

*Dipartimento di Elettronica e Telecomunicazioni, Politecnico di Torino, Italy. Email: giuseppe.calafiore@polito.it

网络定位领域，[redacted]也提出了半定规划（SDP）松弛，[7, redacted]研究了二阶锥（SOC）松弛，而[redacted]则提出了一阶锥方法，并考虑了锚点位置的不确定性。另一种较为经典的方法是采用高斯-牛顿算法等迭代方法直接求解非凸优化问题，例如[redacted]。此外，众所周知，通过对测量方程两两作差，可以将平方距离测量方程转化为一组线性方程，从而消去二次项，例如[redacted]。随后可通过线性最小二乘法求解得到的线性方程组。

Within the wireless localization community, [redacted] also proposed a semidefinite programming (SDP) relaxation approach, while [redacted] proposed a first-order cone programming (SOCP) relaxation approach. A more general SOCP relaxation is studied in [23] where second-order cone (SOC) constraints are considered, and in [19], where a SOC approach is proposed considering also uncertainty on the anchors' locations. A more classical approach is also to solve directly the nonconvex optimization problem by means of iterative methods such as the Gauss-Newton algorithm, see, e.g., [9, 31]. Also, it is well known that squared distance measurement equations can be transformed into a set of *linear* equations by taking pairwise differences between equations, which makes the quadratic terms elide, see, e.g., [11, 17]. The resulting set of linear equations can then be solved via linear Least Squares.

这些已知的定位方法通常将对测量噪声的随机描述，并假设噪声服从已知的统计分布。此外，这些方法都着重计算未知位置的单个点估计。然而，在许多实际场景中，噪声特性可能并不确定，或难以准确建模，从而导致定位性能下降。此外，实际应用中可能不仅需要计算点估计，还希望根据测量信息以及关于噪声特性的先验知识，估计目标物体可能所在的整个空间区域。

Those well known localization methods usually assume a random description of the measurement noise, and assume knowledge of the noise statistical distribution. Further, they all focus on computing *one single* point estimate of the unknown location. In many practical scenarios, however, noise characteristics may be uncertain or difficult to model accurately, and this may lead to degraded localization performance. Further, it may be of practical interest not only to compute a point estimate, but actually to estimate an entire region in space in which the object of interest may be located, based on the measurements information and on the a-priori knowledge on the noise characteristics.

本文探讨一种用于定位的集合成员方法，该方法提供了一组不依赖概率假设的替代框架。相反，它假设测量误差位于已知区间内，从而能够基于集合的分析定位问题。与完整描述误差分布的随机模型相比，误差区间在实践中通常更容易、更自然地获得，更多讨论请参见下文备注1。集合成员方法利用集合论和基于约束的表述，估计目标物体能够确定所在的区域，而非仅给出点估计。这种保证使集合成员定位对于需要稳健、可靠的位置估计的安全关键型应用尤其具有吸引力。

In this paper we explore a set-membership approach, *bounding* approach, or *interval* approach, to localization. In contrast to probabilistic methods, which require knowledge of the measurement noise distribution, set-membership methods only assume that measurement errors lie within known intervals—allowing for a set-based analysis of the localization problem. Error intervals are indeed more easily and naturally obtainable in practice than a full stochastic description of the error distribution, see Remark 1 below for further discussion. By leveraging set theory and constraint-based formulations, the set-membership approach provides estimates of the *region* where the target object is guaranteed to reside, rather than merely a point estimate. Such guarantees make set-membership localization particularly attractive for safety-critical applications requiring robust and reliable position estimation.

关于通过多边定位实现定位的集合成员方法，相关文献似乎相当有限。例如，[redacted]的方法仅限于二维定位，并提出了一种基于接收信号强度指示（RSSI）的分布式集合成员滤波，以动态降低定位误差。在[redacted]中，作者提出了一种集合成员方法，用于提高二维可见光定位系统的位置精度和稳定性，该方法通过一种计算量很大的、基于区间分析的集合反演算法求解。与我们的方法更为接近的是[redacted]中的作者考虑了测量方程中的区间误差，并寻求使所有可行位置上的最坏情况估计误差最小的位置估计：也就是说，在所有与误差界相容的位置中进行寻求。由此得到的问题是一个非凸优化问题，通过半定松弛技术求解。然而，[redacted]中的方法虽然考虑了区间误差和最坏情况误差，但仅旨在计算单个点估计，并且基于通过此方法处理的非凸问题表述。

Literature on set-membership localization approaches, or bounding approaches, is rather limited, however. For instance, [redacted] proposed a set-membership filtering approach for distributed and dynamic reduction of localization errors in wireless sensor networks. In [26] the authors propose a set-membership approach to improve the positioning accuracy and stability of a Visible Light Positioning system in two dimensions, which is solved by means of a computationally-intensive interval analysis-based set inversion algorithm. Closer to our approach, in [21] the authors consider interval errors in the measurements and then solve the problem of finding the smallest circle that contains the intersection of circular rings. The method in [redacted] although considers interval errors and worst-case errors, is still aimed at computing one single point estimate, and it is based on nonconvex problem formulations that are dealt with by means of relaxations.

In this paper, we will first consider the problem of finding the smallest circle that contains the intersection of circular rings, and then we will consider the more general problem of finding the smallest region that contains the intersection of annuli in arbitrary dimension. We will show that these problems are equivalent and lead to a unified model of the form (2.3) which also accommodates both absolute (additive) and relative (multiplicative) error terms. Based on this general model, the m nonlinear equations related to the distance or squared distance measurements from a point x to the m beacons are transformed into a set of $p = m(m-$

在本研究中，我们首先指出，在区间误差和最坏情况误差下，普通距离测量方程与平方距离测量方程是等价的，并可导出形式为(2.3)的统一模型，该模型也兼容绝对（加性）误差项和相对（乘性）误差项。基于这一般模型，与点 x 到 m 个信标的距离或平方距离测量相关的 m 个非线性方程，可转换为一组 $p = m(m-$

1) 22 linear equations. These equations are obtained by pairing the original equations in such a way that the quadratic terms cancel out. Then, we linearize the resulting linear equations around the initial guess, and we solve the resulting linear system in the least-squares sense. In Section 3 we characterize explicitly a convex localization set $\mathcal{X}$ that is guaranteed to contain the original set $\mathcal{X}_{\text{true}}$ of all point consistent with the original nonlinear measurement equations. Then, in Section 4 we show how to compute a maximal ellipsoid inscribed in $\mathcal{X}$; the center of such ellipsoid can be taken as a central estimate of the unknown target's position. Notably, such inscribed ellipsoid can be computed efficiently via convex programming; in particular, we need to solve a convex second-order cone program (SOCP) for finding an inscribed ball which is a particular case of ellipsoid. The key Section 5 discusses instead how we can compute *outer* bounding sets for $\mathcal{X}$, and hence for $\mathcal{X}_{\text{true}} \subseteq \mathcal{X}$. We discuss in particular a simple technique for computing a bounding box $\mathcal{U} \supseteq \mathcal{X}$ via SOCP, and a technique for computing a bounding ellipsoid via SDP. Further aspects are then investigated in Section 6. In particular, Section 6.1 discusses a local approximation approach based on convex quadratic programming for seeking a point in $\mathcal{X}_{\text{true}}$, while Section 6.2 discusses how we can deal with the issue of outliers or error realizations that do not respect the assumed bounds. Although many practical localization problems are posed in two-dimensional or three-dimensional spaces, we remark that the methodology proposed in the present paper works in spaces of any finite dimension. The proposed approach is tested numerically on random scenarios in Section 7. Conclusions are drawn in Section 8.

1.1. Further discussion on related work

Some contributions in the literature consider models that are somewhat related but distinct from the one proposed in the present paper. For example, Yu et al. [30] introduced Ellipsoid SLAM, where location uncertainty is modeled via bounding ellipsoids in the SLAM context, demonstrating the inadequacy of Gaussian noise assumptions in many real-world scenarios and the effectiveness of an unknown-but-bounded (UBB) approach. The SLAM problem discussed in [30], however, is substantially different from the one we discuss in the present paper. Indeed, SLAM is based on recursive linearization, and hence approximation, of the state and measurement equations. Linearization is a local approximation, which in fact uses the measurements to determine the point where to perform the linearization. In this case, the measurement equation depends on the distance from acoustic sources according to the sum of inverse power laws, and the measurement error is assumed to be bounded in a given interval. A bounding ellipsoid is computed for each source based on linearization of the measurement equation and conservative on-line bounding of the linearization residual.

Zhang et al. [31] proposed the use of zonotopes (a particular type of polytopes) rather than ellipsoids for bounding the set of state estimates. Their approach is theoretically appealing, but it is restricted to linear dynamical systems, and thus can not deal with nonlinear measurement models such as the one arising in the multilateration context we discuss in this paper. Wang et al. [24] deal with ellipsoidal state estimation in a nonlinear setting, but instead of classical linearization they propose the reformulation of the

状态界定问题重新表述为一个半无限优化问题，再通过约束采样近似求解，因此同样缺乏状态包含的形式化保证。

This method handles the state estimation problem as a set-membership estimation problem, and then approximately solves the resulting semi-infinite optimization problem via constraint sampling, thus again lacking formal guarantees of state containment.

这个方法处理动态状态估计，并基于逆向局部近似（线性化）来解决集合隶属估计问题。它们都要求提供一个“初始猜测”定位集，例如以椭球的形式，从而启动线性化过程。本文所研究的问题则从全局角度处理定位问题，且没有可用于执行线性化方法的初始猜测。从某种意义上说，本文讨论的方法可视为一种用于确定递归式线性化方法所需初始定位集的技术。

This method handles the state estimation problem as a set-membership estimation problem, and then approximately solves the resulting semi-infinite optimization problem via constraint sampling, thus again lacking formal guarantees of state containment.

其中 ϵ 的上界和下界取决于具体的模型和误差类型（绝对误差或相对误差）。特别地，很容易验证：- 对于具有绝对误差的模型 (2.1)，有

- For model (2.1) with absolute errors, it holds that

$$[redacted] \quad [redacted], \quad [redacted] \quad [redacted], \quad [redacted].$$

- 对于具有相对误差的模型 (2.1)，有

- For model (2.1) with relative errors, it holds that

$$[redacted] \quad [redacted], \quad [redacted], \quad [redacted], \quad [redacted] \quad [redacted].$$

- 对于具有绝对误差的模型 (2.2)，有

- For model (2.2) with absolute errors, it holds that

$$[redacted] \quad [redacted], \quad [redacted], \quad [redacted], \quad [redacted].$$

- 对于具有相对误差的模型 (2.2)，有

- For model (2.2) with relative errors, it holds that

$$[redacted] \quad [redacted] \quad [redacted], \quad [redacted], \quad [redacted], \quad [redacted].$$

We let [redacted] ξ^* 分别表示包含条目 ϵ, ϵ [redacted] 的向量，其中 [redacted] ξ_i, ξ_i^+ 表示超矩形 $i = 1, \ldots, m$, and we let H denote the hyperrectangle

$$[redacted] \quad [redacted] \quad [redacted] \quad [redacted].$$

In the sequel, we focus on the general model (2.3), which is the representation of all four measurement models discussed above. According to (2.3), each measurement confines the possible locations x in a hyperspherical shell region

$$\mathcal{S}_i = \{x \in \mathbb{R}^n : \sqrt{\xi_i^-} \le \|x - a^{(i)}\|_2 \le \sqrt{\xi_i^+}\}. \tag{2.9}$$

包含所有与全部不确定测量相容的 x 位置的集合 Xtrue，是各个 $\mathcal{S}_i$ 区域的交集：

$$[redacted] \quad [redacted] \quad [redacted].$$

Xtrue 通常是一个非凸集，图展示了 R? set 的一个示例，其中有三个锚点，每个 $\mathcal{S}_i$ 都是 $\mathbb{R}^2$ 个圆环域。

备注1（区间噪声模型）。例如，当已知物理传感器误差限，或测量设备提供了认证精度或分辨率时，对测量误差采用未知但有界的假设是合适的。例如，具有 [redacted] cm 重复性的激光雷达测距传感器，参见 [redacted]，误差界可以根据底层传感器机制的物理原理或制造商校准证书严格推导得出，参见 [redacted]。此外，在无法可靠确定噪声分布的情况下（例如非平稳传感器、老化设备、变化的环境），与假设测量误差服从高斯分布相比，采用确定性界限更为可信。这在系统辨识的早期阶段或环境条件波动的野外机器人学中十分常见。实践中，可以根据校准数据、制造商规格或截断统计模型（例如，30个高斯界限）获得误差界。

Remark 1 (Interval noise model). For example, when the measurement error is appropriate for instance when one has physical sensor error limits, or when the measurement device provides a certified accuracy or resolution, e.g., a LiDAR range sensor with ±3cm repeatability, see, e.g., [22, 15]. Error bounds can be rigorously derived from the physics of the underlying sensor mechanisms or from manufacturer's calibration certificates, see, e.g., [4]. Also, in situations in which one cannot confidently identify a noise distribution (nonstationary sensors, aging equipment, variable environments), a deterministic bound is more credible than assuming, say, Gaussianity of the measurement errors. This is typical in early-stage system identification or in field robotics where environmental conditions fluctuate. In practice, bounds on errors can be obtained from calibration data, manufacturer specifications, or from truncated statistical models (e.g., 3σ Gaussian bounds).

[redacted]

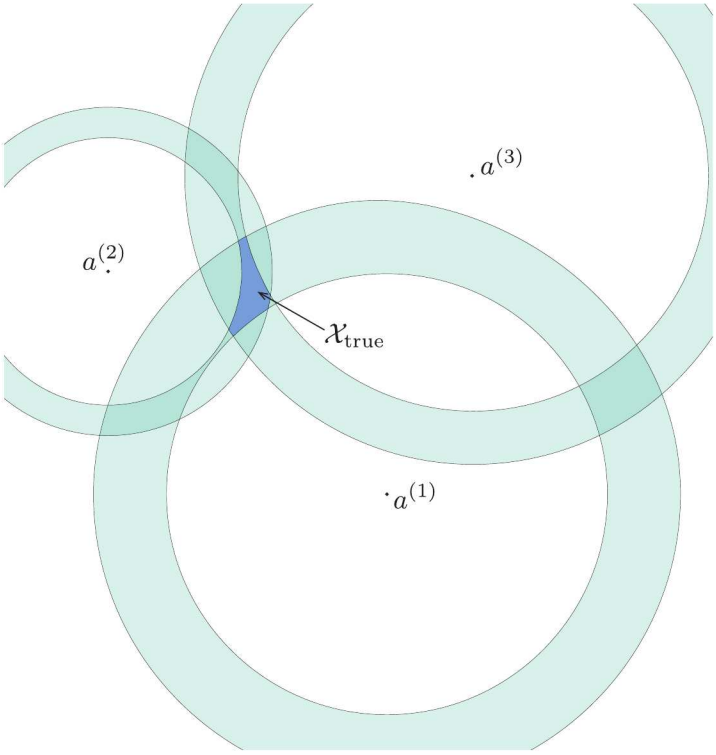

Fig. 1. 在 $\mathbb{R}^2$ 中使用三个锚点进行定位。 *Localization using three anchors in* $\mathbb{R}^2$.

In safety-critical systems (aerospace, autonomous driving, process control) one needs to guarantee that the uncertainties in the measurements will not cause the system to violate safety constraints. In such cases, UBB models can be used to prove that safety requirements are met for all noise realizations within the bounds, a statement which is not obtainable via purely stochastic models. In our context, the use of UBB noise and a set-membership approach leads to deriving an outer bounding set which is *guaranteed* to contain our localization target.

在安全关键系统（航空航天、自动驾驶、过程控制）中，需要确保任何可容许噪声实现不会导致系统违反安全约束。在这类情况下，UBB模型可以证明，对于所有噪声实现，该性质均成立；仅依靠随机模型无法得出这一结论。在我们的情境中，采用UBB噪声和集合成员方法，可以推导出一个外包集合，并保证该集合包含我们的定位目标。

We also remark that the specific interval UBB model used in eqs. (2.1), (2.2) is well suited to our context. In fact, assuming in (2.1) and (2.2) that the measurement errors belong to independent intervals is natural (or, at any rate, less restrictive) if the errors are independent from one another, since they depend only on the characteristics of the distance measurement device, and this is reflected well in the assumptions that they lie in independent intervals. An ellipsoidal model for the measurement errors would instead imply a mutual dependence among the measurement errors (e.g., the amplitude of errors $\epsilon_1, \ldots, \epsilon_{m-1}$ constrains the amplitude of error ϵ_m), which would be unnatural in our context. ⋆

我们还指出，与椭球UBB误差模型相比，式(2.1)–(2.2)中使用的特定区间UBB模型更适合我们的情境。事实上，假设式(2.1)或(2.2)中的测量误差彼此独立很自然，因为它们仅取决于距离测量设备的特性，而假设这些误差分别位于互相独立的区间内，恰好体现了这一点。相反，测量误差的椭球模型意味着各测量误差之间相互依赖（例如，误差 $\epsilon_1, \ldots, \epsilon_{m-1}$ 的幅度会限制误差 ϵ_m 的幅度），这在我们的情境中并不自然。⋆

In the next section, we introduce a set-valued, outer bounding set, that provides a certified outer bound for the true feasible set $\mathcal{X}_{\text{true}}$ of locations compatible with the uncertain measurements (note that $\mathcal{X}_{\text{true}}$ is in general nonconvex). Specifically, $\mathcal{X}$ is defined as the intersection of the m measurement closed balls and the difference-of-measurements (d.o.m.) polyhedron $\mathcal{X}_d$.

在下一节中，我们将介绍一个集值外包区域，称为定位集，它为与不确定测量相兼容的位置的真实可行集 $\mathcal{X}_{\text{true}}$ 提供经认证的外部界（注意，$\mathcal{X}_{\text{true}}$ 通常是非凸的）。具体而言，$\mathcal{X}$ 定义为 m 个测量闭球与测量差（d.o.m.）多面体 $\mathcal{X}_d$ 的交集。

3. 测量差（comparison）对应的图和定位集 the graph and localization set

3.1. 测量差图 Differences of measurements. 注意，第 i 个测量方程 (2.3) 可展开为 We observe that the ith measurement equation (2.3) can be expanded to

$$[illegible]$$

然后，将第 j 个测量方程从第 i 个测量方程中相减，对于 $i \neq j$，我们得到 Then, subtracting the jth measurement equation from the ith, for $i \neq j$, we obtain that

$$[illegible]$$
$$= \xi_i - \xi_j,$$

其中可以看到，x 中的一次项消失了。接着考虑所有成对的测量方程，对于 $i, j = 1, \ldots, m$，可得到 $p = m(m-1)/2$ 个关于 x 的线性方程，其形式为 where we see that the linear terms in x have canceled. Considering pairs of measurement equations for $i, j = 1, \ldots, m$, we obtain $p = m(m-1)/2$ linear equations in x of the form

$$[illegible]$$

对于所有 $i, j = 1, \ldots, m$，$i < j$。我们假设这已经是一般性的，即没有丢失一般性，因为 p 对 (i, j) 可以按字典序排列为 $(1, 2), (1, 3), \ldots, (1, m), (2, 3), \ldots, (2, m), \ldots, (m-1, m)$。接下来定义 for all $i, j = 1, \ldots, m$, $i < j$. We assume without loss of generality that the p pairs (i, j) are ordered as $(1, 2), (1, 3), \ldots, (1, m), (2, 3), \ldots, (2, m), \ldots, (m-1, m)$. We next define

$$[illegible]$$

其中 $E \in \mathbb{R}^{p,m}$ 是一个矩阵，其第 k 行的形式为 $(e_i - e_j)^\top$，其中 $e_i \in \mathbb{R}^m$ 是第 i 个标准基向量（即除位置 i 为 1 外，其余元素均为 0）。可见，(i, j)，$i < j$ 构成第 k 对锚点。 where $E \in \mathbb{R}^{p,m}$ is a matrix whose kth row has the form $(e_i - e_j)^\top$, where $e_i \in \mathbb{R}^m$ is the ith standard basis vector (i.e., the vector with a 1 in position i), and (i, j), $i < j$, form the kth pair of anchors.

3.2. 测量图 The measurement graph. 我们的问题结构有一种自然的图论解释：m 个锚点构成图的顶点，每当我们考虑相应的测量值之差 (3.1) 时，就说存在一条从节点 j 指向 i 的边 (i, j)。因此，考虑所有 i 对应的测量值之差 (3.1)，便构成一个具有 m 个顶点和 $p = m(m-1)/2$ 条边的连通图 G。根据定义，$E \in \mathbb{R}^{m,p}$ 表示该图的关联矩阵。 The structure of our problem has a natural graph theoretic interpretation: the m anchors form the vertices of a graph, and we say there is an edge (i, j) from node j to i whenever we consider the corresponding difference of measurements eq. (3.1). Considering all difference of measurements (i, j) for all $j > i$ thus forms a connected graph $\mathcal{G}$ with m vertices and $p = m(m-1)/2$ edges. We observe that, according to its definition, $E^\top \in \mathbb{R}^{m,p}$ represents the incidence matrix of such graph. ⋆

Setting

$$[illegible]$$

可以验证，方程 (3.1) 可简洁地改写为 One can verify that (3.1) can be rewritten compactly as

$$2EA^\top x = E\omega - \nu, \quad \nu = E\xi \tag{3.3}$$

where

$$EA^\top = \begin{bmatrix} (a^{(1)} - a^{(2)})^\top \\ \vdots \\ (a^{(m-1)} - a^{(m)})^\top \end{bmatrix}, \; E\omega = \begin{bmatrix} \|a^{(1)}\|_2^2 - \|a^{(2)}\|_2^2 \\ \vdots \\ \|a^{(m-1)}\|_2^2 - \|a^{(m)}\|_2^2 \end{bmatrix}.$$

3.2. Difference-of-measurements polyhedral sets. We next characterize a convex polyhedral set[1] that is guaranteed to contain $\mathcal{X}_{\text{true}}$.

命题 3.1. *Let $V = \{\nu \in \mathbb{R}^m : \exists \xi \in \mathbb{R}^n, \nu = E\xi, H\xi \leq h\}$. The set*

$$\mathcal{X}_d = \{x \in \mathbb{R}^n : Ax = \nu, \nu \in V\}$$

is a polyhedron, and it contains $\mathcal{X}_{\text{true}}$, i.e., that $\mathcal{X}_{\text{true}} \subseteq \mathcal{X}_d$.

证明. 首先注意，根据定义，对于任意 $x \in \mathcal{X}_{\text{true}}$，存在某个 $\xi \in H$，使得式 (2.3) 均成立，因此，式 (2.3) 推导出的相对差分方程 (3.1) 也成立，这意味着 $x \in \mathcal{X}_d$，从而 $\mathcal{X}_{\text{true}} \subseteq \mathcal{X}_d$。下来注意，$V$ 是一个多胞体，因为它是超矩形 H 经线性映射所得的像，参见例如 [13]。同理，$\mathcal{X}_d$ 是一个多面体，因为它是某个多胞体经仿射映射所得的原像，参见例如 [6] 中的习题 3.9。□

Proof. The first observation that follows directly from the definition of $\mathcal{X}_{\text{true}}$ is that (2.3) holds for some $\xi \in H$, which implies that (3.1) also holds, which means that $x \in \mathcal{X}_d$. Next, observe that V is a polytope, since it is the image of the hyperrectangle H through a linear map, see, e.g., [13]. Similarly, $\mathcal{X}_d$ is a polyhedron since it is the preimage of a polytope through an affine map, see, e.g., ex. 3.9 in [6]. □

如命题 3.1 所述，集合 $\mathcal{X}_d$ 可通过一组线性等式与不等式刻画为 $\mathcal{X}_d = \{x \in \mathbb{R}^n : \exists \xi \in H, Ax = E\xi, H\xi \leq h\}$。在 V 中寻找一个点，或确定不存在这样的点，相当于求解一个线性规划 (LP) 可行性问题。注意，虽然 $\mathcal{X}_d$ 属于正交集 H，也就是说，ξ 的各个元素彼此相互独立，但对于 $\nu = E\xi$，其各项之间存在相关关系，因此，V 并非如此，其各项彼此相互依赖，从而也给出 V 的另一种描述，即 V 是 ξ 的各项均在独立区间内有界，也就是说，ξ 的元素均在独立区间内有界，但对于 $\nu = E\xi$，其各项之间存在相关关系，因此，V 并非如此，其各项彼此相互依赖，从而也给出 V 的另一种描述，即 V 是一个 polytope，因为它是超矩形 H 经线性映射所得的像，参见例如 [13]。同理，$\mathcal{X}_d$ 是一个多面体，因为它是某个多胞体经仿射映射所得的原像，参见例如 [6] 中的习题 3.9。□

As mentioned in Remark 2, matrix E represents the (transpose) incidence matrix of a measurement graph G. Since G is connected, $\operatorname{rank}(E) = n - 1$, see, e.g., Lemma 2.2 in [3]. Now suppose first that $\nu \in V$. Then, $\nu = E\xi$ for some ξ, which implies $\nu \in \mathcal{R}(E)$, and all ξ compatible with this equation are parametrized by $\xi = E^\dagger \nu + \alpha \mathbf{1}$ for $\alpha \in \mathbb{R}$, therefore it must be $E^\dagger \nu + \alpha \mathbf{1} \in H$ for some α, which implies that $\nu \in \tilde{V}$. Conversely, suppose $\nu \in \tilde{V}$. Then, $\nu \in \mathcal{R}(E)$ and we define $\xi = E^\dagger \nu + \alpha \mathbf{1} \in H$, for which it holds that

$$E\xi = EE^\dagger \nu + \alpha E\mathbf{1} = \nu,$$

since $\mathbf{1}$ is in the nullspace of E, and $EE^\dagger$ is the orthogonal projection onto $\mathcal{R}(E)$, so $EE^\dagger \nu = \nu$ because $\nu \in \mathcal{R}(E)$. Therefore $\nu \in V$; we showed that V and $\tilde{V}$ coincide. □

命题 3.2. *Let $V = \{\nu \in \mathbb{R}^m : \exists \xi \in H, \nu = E\xi\}$ and $\tilde{V} = \{\nu \in \mathbb{R}^m : \exists \alpha \in \mathbb{R}, E^\dagger \nu + \alpha \mathbf{1} \in H\}$. Then, $V = \tilde{V}$.*

证明. 如注 2 中所述，矩阵 $E \in \mathbb{R}^{m \times n}$ 表示测量差分图 G 的（转置）关联矩阵。由于该图连通，因此 $\operatorname{rank}(E) = n - 1$，其零空间为 $\mathcal{N}(E) = \{\alpha \mathbf{1} : \alpha \in \mathbb{R}\}$，参见例如 [3] 中的引理 2.2。现在，先假设 $\nu \in V$。那么 $\nu = E\xi$，其中 ξ 满足该式，这意味着 $\nu \in \mathcal{R}(E)$，而所有与该等式相容的 ξ 都可参数化为 $E^\dagger \nu + \alpha \mathbf{1}$，其中 $\alpha \in \mathbb{R}$，因此，对某个 α，必有 $E^\dagger \nu + \alpha \mathbf{1} \in H$，这意味着 $\nu \in \tilde{V}$。反过来，假设 $\nu \in \tilde{V}$。那么 $\nu \in \mathcal{R}(E)$，并定义 $\xi = E^\dagger \nu + \alpha \mathbf{1} \in H$，此时有

$$E\xi = EE^\dagger \nu + \alpha E\mathbf{1} = \nu,$$

由于 $\mathbf{1}$ 属于 E 的零空间，且 $EE^\dagger$ 是投影到 $\mathcal{R}(E)$ 上的正交投影算子，而 ν 已经位于 $\mathcal{R}(E)$ 内，因此投影结果与 ν 相同，由此证明 $\nu \in V$，这就完成了 V 与 $\tilde{V}$ 相同的证明。□

Proof. As mentioned in Remark 2, matrix $E \in \mathbb{R}^{m \times n}$ represents the (transpose) incidence matrix of a measurement graph G. Since G is connected, $\operatorname{rank}(E) = n - 1$, see, e.g., Lemma 2.2 in [3]. Now suppose first that $\nu \in V$. Then, $\nu = E\xi$ for some ξ, which implies $\nu \in \mathcal{R}(E)$, and all ξ compatible with this equation are parametrized by $\xi = E^\dagger \nu + \alpha \mathbf{1}$ for $\alpha \in \mathbb{R}$, therefore it must be $E^\dagger \nu + \alpha \mathbf{1} \in H$ for some α, which implies that $\nu \in \tilde{V}$. Conversely, suppose $\nu \in \tilde{V}$. Then, $\nu \in \mathcal{R}(E)$ and we define $\xi = E^\dagger \nu + \alpha \mathbf{1} \in H$, for which it holds that

$$E\xi = EE^\dagger \nu + \alpha E\mathbf{1} = \nu,$$

since $\mathbf{1}$ is in the nullspace of E, and $EE^\dagger$ is the orthogonal projection onto $\mathcal{R}(E)$, so $EE^\dagger \nu = \nu$ because $\nu \in \mathcal{R}(E)$. Therefore $\nu \in V$; we showed that V and $\tilde{V}$ coincide. □

命题 3.3. *The set $\mathcal{X}_d$ is given by*

$$\mathcal{X}_d = \{x \in \mathbb{R}^n : \exists \alpha \in \mathbb{R}, Ax = E^\dagger \nu + \alpha \mathbf{1}, E^\dagger \nu + \alpha \mathbf{1} \in H\}$$

where

$$E^\dagger \nu + \alpha \mathbf{1} = \begin{bmatrix} \nu_{12} + \alpha \\ \nu_{13} + \alpha \\ \vdots \\ \nu_{1n} + \alpha \end{bmatrix}.$$

证明. 根据定义，$\mathcal{X}_d = \{x \in \mathbb{R}^n : Ax = \nu, \nu \in V\}$，应用命题 3.2，可得到等价表示

Proof. By the definition, $\mathcal{X}_d = \{x \in \mathbb{R}^n : Ax = \nu, \nu \in V\}$, applying Proposition 3.2 we obtain the equivalent representation

$$\mathcal{X}_d = \{x \in \mathbb{R}^n : \exists \alpha \in \mathbb{R}, Ax = E^\dagger \nu + \alpha \mathbf{1}, E^\dagger \nu + \alpha \mathbf{1} \in H\}$$

$$E^\dagger \nu + \alpha \mathbf{1} = \begin{bmatrix} \nu_{12} + \alpha \\ \nu_{13} + \alpha \\ \vdots \\ \nu_{1n} + \alpha \end{bmatrix}.$$

满足，这可通过线性规划检验的条件。因为这相当于寻找 $\mathcal{C}$ 中 U 的列构成 $\mathcal{V}(AE)$ 的一组基，且 $\mathcal{R}(EA) \cap \mathcal{N}(AE) = \{0\}$。注意，如果测量值确实是由某个真实位置 x_{true} 对应的模型方程 (2.1) 或 (2.2) 生成的，并且噪声项符合其界限，那么至少必然存在一个点属于 $\mathcal{X}_{\text{true}}$（$x_{\text{true}}$ 本身），因此 $\mathcal{X}_d$ 非空，进而 $\mathcal{Y}_d$ 非空。因此，$\mathcal{Y}_d$ 非空性失效的唯一可能是某个测量值不符合假定的模型方程，或者误差界未得到满足，在实际中，存在离群值、意外误差或测量设备故障时，就可能发生这种情况。关于如何处理这种情况，参见第6节。

Since the left-hand side of the above equation is in $\mathcal{R}(EA^\top)$ while the right-hand side is in $\mathcal{R}(E)$, and it holds in general that $\mathcal{R}(EA^\top) \subseteq \mathcal{R}(E)$, we have that $\mathcal{X}_d$ is *nonempty* if and only if

$$\mathcal{R}(E) \subseteq \mathcal{R}(EA^\top) \quad \Leftrightarrow \quad \mathcal{R}(E) = \mathcal{R}(EA^\top). \tag{3.5}$$

如果式 (3.5) 成立，则 $\mathcal{Y}_d$ 非空，因为显然在这种情况下，x 可以沿着 $\mathcal{V}(EA)$ 中的任意方向无限暗长。因此，EA 满秩这一条件可保证 $\mathcal{Y}_d$ 有界（进而 $\mathcal{X}_{\text{true}}$ 也有界）。特别要注意，在 $m \geq n$ 且 $\operatorname{rank}(EA^\top) = n$ 这一特殊但常见的情况下，$\mathcal{R}(EA^\top) = \mathcal{R}(E)$，因此 $\mathcal{Y}_d$ 必定有界且非空。$\star$

If (3.5) holds, then $\mathcal{N}(EA^\top) = \mathcal{N}(A)$, and so $\mathcal{V}(EA^\top) = \mathcal{V}(A)$, which is assumed trivial in such cases since error terms are generated along every direction in $\mathcal{N}(EA^\top)$. Thus, the condition that $EA^\top$ has full rank guarantees boundedness of $\mathcal{Y}_d$ (and hence of $\mathcal{X}_{\text{true}}$). Notice in particular that in the special but common case when $m = n + 1$ and $\operatorname{rank}(EA^\top) = n$ then $\mathcal{R}(EA^\top) = \mathcal{R}(E)$, hence $\mathcal{X}_d$ is surely bounded and nonempty. $\star$

备注 3.4（标准条件）我们关注的典型情形是 $m \geq n$ 且 $m \approx n$，也就是说，锚点的数量大于空间维数，这一假设确保 $p \geq m(m+1)/2 - n + 1$，从而矩阵 $A \in \mathbb{R}^{p,n}$ 和 $E \in \mathbb{R}^{p,m}$ 都是“高”矩阵。我们通常还假设锚点处于一般位置，因此 $EA^\top$ 满列秩，即 $\operatorname{rank}(EA^\top) = n$，如前一条注释所述，这可保证 $\mathcal{Y}_d$ 有界。$\star$

Remark 3.4 (Standard conditions) The typical situation we are interested in is when $m \geq n$ and $m \approx n$, that is, the number of anchors is larger than the space dimension. This assumption ensures that $p \geq m(m+1)/2 - n + 1$, so that matrices $A \in \mathbb{R}^{p,n}$ and $E \in \mathbb{R}^{p,m}$ are "tall" matrices. We also typically consider anchors that are in general position, so that $EA^\top$ is full column rank, i.e., $\operatorname{rank}(EA^\top) = n$, which guarantees boundedness of $\mathcal{X}_d$, as mentioned in the previous remark. $\star$

3.3. The localization set. In practice, we usually have additional information about the position x we are trying to localize. For example, we usually know that x is contained in a certain region of space, or that it is relatively close to a certain point. This information can be incorporated in the definition of $\mathcal{X}_d$ by intersecting it with a set $\mathcal{H}$ that represents our prior knowledge about x. We call $\mathcal{H}$ the *localization set*. In this section we describe a simple and common choice for $\mathcal{H}$, namely, an intersection of balls centered at the anchors. Other choices are discussed briefly in Section 3.4.

3.3. 定位集。实际中，我们通常还有关于待定位位置 x 的额外信息。例如，我们通常知道 x 位于空间的某个特定区域内，或者知道它相对接近某个特定点。这些信息可以通过将 $\mathcal{X}_d$ 与一个表示我们对 x 的先验知识的集合 $\mathcal{H}$ 相交来纳入 $\mathcal{X}_d$ 的定义中。我们将 $\mathcal{H}$ 称为*定位集*。本节描述 $\mathcal{H}$ 的一个简单且常见的选择，即以锚点为中心的球的交集。$\mathcal{H}$ 的其他选择将在3.4节中简要讨论。

Recall that $\mathcal{X}_{\text{true}}$ is also contained in a convex region $\mathcal{H}$ given by intersection of m closed balls

$$\mathcal{H} = \bigcap_{i=1}^{m} \{x \mid \|x - a_i\|_2 \leq \sqrt{\rho_i}\} = \{x \mid \|x - a_i\|_2^2 \leq \rho_i, \ i = 1, \ldots, m\}. \tag{3.6}$$

Defining

$$\mathcal{X} = \mathcal{X}_d \cap \mathcal{H} = \{x \mid \|Ax - d\|_\infty \leq \varepsilon, \ \|x - a_i\|_2^2 \leq \rho_i, \ i = 1, \ldots, m\}, \tag{3.7}$$

我们有 Virue CX，因此称 ¥ 为定位集。该集合为含噪测量方程(2.3)的可能解的真实(非凸)集合 Vrue 提供了紧外包，并细化了由 wq 给出的外界。The Virue C ¥ 的紧致程度取决于锚点配置、目标位置和噪声界限。本文不给出关于外包紧致性的形式化结果。然而，数值实验表明，当锚点在目标周围分布良好时，¥ 通常几乎与 Vue 重合，而接近共线、共面或聚集锚点会增加保守性。这一事实的示例见图2和图3。比值 vol(¥)/ vol(Atrue) 为该保守性提供了一个有用的度量，并在第7节的数值实验中进行了估计。

The tightness of the bounding $\mathcal{X} \subset \mathcal{X}$ depends on anchors' configuration, target position and noise bounds. We do not provide formal results on the bounding tightness in this paper. However, numerical experiments shows that $\mathcal{X}$ typically becomes nearly coincident with $\mathcal{X}_{\text{true}}$ when anchors are well distributed around the target, while near colinear or coplanar or clustered anchors increase conservativeness, see an exemplification of this fact in Figure 2 and Figure 3. The ratio $\text{vol}(\mathcal{X})/\,\text{vol}(\mathcal{X}_{\text{true}})$ provides a useful measure of this conservativeness and it is estimated in the numerical experiments of Section 7.

图2展示了 R2 中包含 cn ■■ 个锚点的 i 个示例，其中灰色多边形表示 Vz，绿色轮廓(红线表示 Vipue，球 H„ 的边界(部分应的球面) 以蓝色表示 drue 定位集 X ■ X4NH 不直接显示在图中，但通过将 Yq 与圆盘 H„ ■■ 1,2,3 取交集，可以很容易地从图中推断出来。

Figure 2 shows two examples in $\mathbb{R}^2$ with m anchors, the polygon $\mathcal{X}_d$ is depicted in gray, the boundary of the balls $\mathcal{H}_i$ (i.e., the corresponding spheres) are depicted in blue. The localization set $\mathcal{X} = \mathcal{X}_d \cap \mathcal{H}$ is not shown directly in the picture, but it can be easily inferred visually by intersecting $\mathcal{X}_d$ with the discs $\mathcal{H}_i$, $i = 1, 2, 3$. Figure 3 shows the same target and relative bounds used in Figure 2, but with one anchor progressively displaced so to worsen the conditioning of the $E4^{\dagger}$ matrix (anchor points tend to be "nearer to colinearity"). We observe that the gray polygon depicting $\mathcal{X}_d$ becomes larger as the anchors' geometry worsens. If the anchors become exactly colinear, $\mathcal{X}_d$ would become unbounded, as discussed in Remark 3. Boundedness of the localization set $\mathcal{X} = \mathcal{X}_d \cap \mathcal{H}$ is however maintained in all cases, due to the intersection of $\mathcal{X}_d$ with the bounded balls $\mathcal{H}_i$, $i = 1, \ldots, m$.

图3展示了与图2中相同的目标和相对界限，但逐步移动其中一个锚点，以恶化 EA 矩阵的条件性（锚点往往变得"更加接近共线"）。我们观察到，表示 Y, 的灰色多边形会随着锚点几何的恶化而变大。如果锚点变得完全共线，Yq 将变得无界，正如注3中所讨论的。然而，在所有情况下，定位集 X ■ XaNH 的有界性都得以保持，这是由于 ¥q 与有界球 H; i ■■ m 的交集所致。

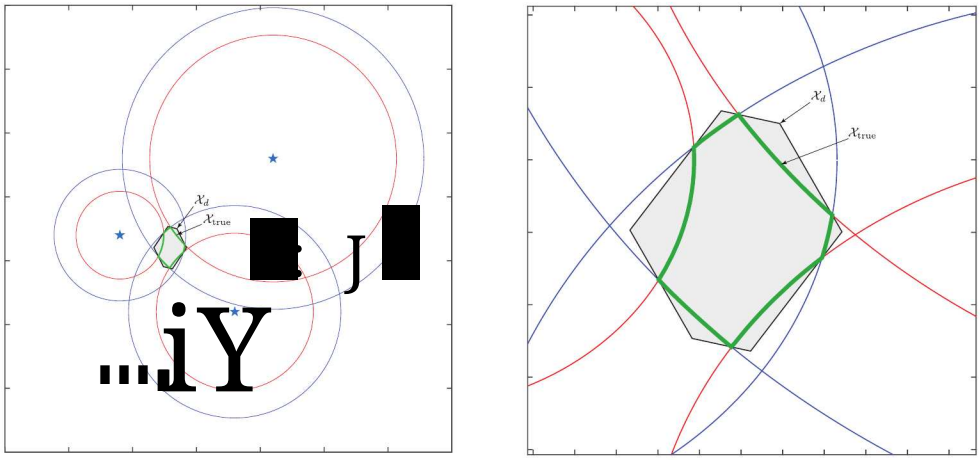

图2. 在一个包含三个锚点的二维示例中，集合 Xtrue（绿色边框）和 Xq（黑色边框并以灰色填充）。左图：完整视图，蓝色和红色表示环形区域；右图：真实的非凸定位集 Xtrue 及其包围多胞体 Xa- 的细

Figure 2. Sets Xq (black frame, filled in gray) and Xtrue (green frame) for a two-dimensional example with three anchors. Left panel: full view with annulus regions depicted in blue and red; Right panel: detail of the true non-convex localization set $\mathcal{X}_{\text{true}}$ and its bounding polytope $\mathcal{X}_d$.

4. Inner approximation of the localization set. 定位集的内近似。接下来，我们讨论如何计算包含在 Y（定位集）中的简单集合，从而得到锚点位置的良好中心估计。由于 ¥ 是真实可行集 Vrue 的凸外界，这些内近似保证位于 V 中，但不一定是 Vrue 的子集。第5节将转而讨论如何找到

4. Inner approximation of the localization set. We next discuss how to compute simple sets included in $\mathcal{Y}$ (the localization set), and hence to obtain convenient central estimates of the location. Since $\mathcal{X}$ is a convex outer bound of the true feasible set $\mathcal{X}_{\text{true}}$, these inner approximations are guaranteed to lie in $\mathcal{X}$, but they are not necessarily subsets of $\mathcal{X}_{\text{true}}$. Section 5 discusses instead the main problem of finding

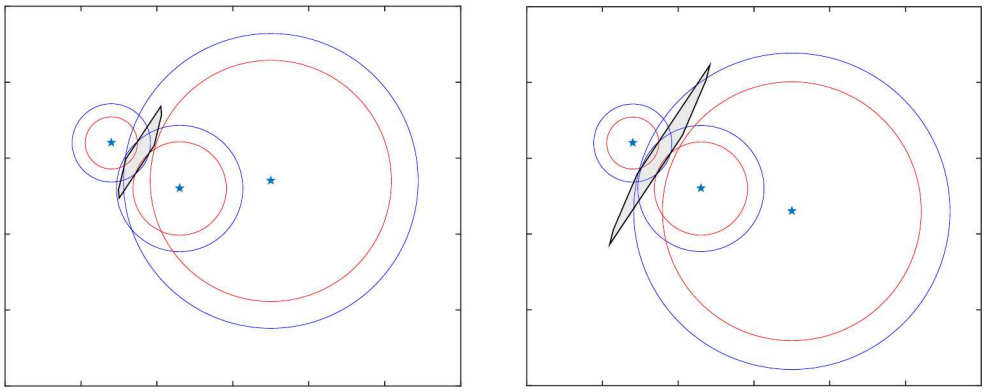

图3：随着最右侧锚点移动，后验估计几何的条件性变差时的*Illustration of how the conditioning of the posterior estimate worsens as the right-most anchor moves so to worsen the conditioning of the anchors' geometry.*

an outer bounding ellipsoid of the true set $\mathcal{X}$, and hence $\mathcal{X}_{\text{true}}$.

4.1 Computing an inscribed ball

Given a polytope $\mathcal{Y}$, we seek to find the largest ball $\mathcal{B}(c,r)$ contained in $\mathcal{Y}$. The central estimate will then be given by the center of such ball. Denoting the ball by

$$\mathcal{B}(c,r) = \{\xi \in \mathbb{R}^n : \xi = c + ru,\ c \in \mathbb{R}^n, \|u\|_2 \leq 1\},$$

where c is the center and r is the radius, we have that $\mathcal{B}(c,r) \subseteq \mathcal{Y} = \{x : Ax \leq b\}$ if and only if $\mathcal{B}(c,r)$ and $\mathcal{Y}$ satisfy the containment relation $\mathcal{B} \subseteq \mathcal{H}$. We next examine these two inclusions separately.

First, using Proposition 3.3 we know that $\mathcal{B}(c,r) \subseteq \mathcal{V}_d$ if for any $x \in \mathcal{B}(c,r)$ there exist $\alpha \in \mathbb{R}$ such that

$$\begin{bmatrix} [A]_1 \\ \vdots \\ [A]_m \end{bmatrix} x \leq \begin{bmatrix} [b]_1 \\ \vdots \\ [b]_m \end{bmatrix} - \alpha \begin{bmatrix} [w]_1 \\ \vdots \\ [w]_m \end{bmatrix},$$

where $[A]_i$ denotes the ith row of A and $[w]_i$ denotes the ith element of the vector w. Now, since $x \in \mathcal{B}(c,r)$, we have that $x = c + ru$ for some u with $\|u\|_2 \leq 1$, hence we can impose the above conditions for all such u, and obtain a conservative estimate. In such case we have that the above conditions hold if there exist α such that for $i = 1, \ldots, m$,

$$[A]_i c + r[A]_i u \leq [b]_i - \alpha [w]_i$$

Since $\max_{\|u\|_2 \leq 1} [A]_i u = \|[A]_i\|_2$ and $\min_{\|u\|_2 \leq 1} [A]_i u = -\|[A]_i\|_2$, the above conditions become explicitly

$$[A]_i c + r\|[A]_i\|_2 \leq [b]_i - \alpha [w]_i$$

因此我们有 $\mathcal{B}(c,r) \subseteq \mathcal{V}_d$ 当且仅当

$$[A]_i c + r\|[A]_i\|_2 + \alpha [w]_i \leq [b]_i, \quad i = 1, \ldots, m,$$

其中 $z \in \mathbb{R}^m$ 满足 $\|z\|_2 \le 1$。然而，如上所述，这些条件是保守的，因为我们对球中的所有点考虑了一个固定的 α，通过允许 α 依赖于 $x = c + ru$，从而依赖于 u，可以改善这一情形（即可以得到更大的内接球）。具体而言，我们考虑如下形式的仿射依赖

where $z \in \mathbb{R}^m$ satisfies $\|z\|_2 \le 1$. However, as discussed above, these conditions are conservative due to the fact that we considered a fixed α for all points in the ball. The situation can be improved (i.e., a larger inscribed ball can be obtained) by allowing α to depend on $x = c + ru$, hence on u. Specifically, we consider an affine dependence of the form

$$\alpha = \alpha_0 + \alpha_1^T u,$$

其中 $\alpha_0 \in \mathbb{R}$ 和 $\alpha_1 \in \mathbb{R}^n$ 是待确定的参数。这种仿射依赖的选择受到[5]的启发，在那里它被证明在保持可处理的问题表述的同时，能够降低保守性。

where $\alpha_0 \in \mathbb{R}$ and $\alpha_1 \in \mathbb{R}^n$ are parameters to be determined. This choice is inspired by [5], where it was shown that such an affine dependence can reduce conservatism while still leading to a tractable problem formulation. The inclusion conditions now become, for $i = 1, \dots, m$,

$$a_i^T (c + ru) + \|A_i (c + ru) - b_i\|_2 \le \alpha_0 + \alpha_1^T u$$

即

That is

$$a_i^T c + \|A_i c - b_i\|_2 + (r a_i^T + r A_i^T (A_i c - b_i)/\|A_i c - b_i\|_2 - \alpha_1)^T u \le \alpha_0$$

像前面一样，最后一个表达式关于 u 的最大值和最小值可得，当 $\|u\|_2 \le 1$ 时，

Proceeding as previously, the maximum and minimum of the last expression with respect to u over $\|u\|_2 \le 1$ are obtained as

$$\max_{\|u\|_2 \le 1} \left(r a_i^T + r A_i^T (A_i c - b_i)/\|A_i c - b_i\|_2 - \alpha_1 \right)^T u = \|r a_i + r A_i^T (A_i c - b_i)/\|A_i c - b_i\|_2 - \alpha_1\|_2$$

$$\min_{\|u\|_2 \le 1} \left(r a_i^T + r A_i^T (A_i c - b_i)/\|A_i c - b_i\|_2 - \alpha_1 \right)^T u = -\|r a_i + r A_i^T (A_i c - b_i)/\|A_i c - b_i\|_2 - \alpha_1\|_2$$

因此，(4.2) 成立当且仅当

Hence, (4.2) holds for $i = 1, \dots, m$, if and only if

$$a_i^T c + \|A_i c - b_i\|_2 + \|r a_i + r A_i^T (A_i c - b_i)/\|A_i c - b_i\|_2 - \alpha_1\|_2 \le \alpha_0$$

对于 $i = 1, \dots, m$ 成立。这些构成了关于决策变量 c、r、α 和 h 的一组凸二阶锥（SOC）约束可保证 $\mathcal{B}(c, r) \subseteq \mathcal{X}_d$。

for $i = 1, \dots, m$. These constitute a set of convex second-order cone (SOC) constraints on the decision variables $c, r, \bar{\alpha}$ and h that guarantee $\mathcal{B}(c, r) \subseteq \mathcal{X}_d$.

接下来，考虑包含关系 $\mathcal{B}(c, r) \subseteq \mathcal{H}$。当且仅当 $\|a_i\|_2 \le b_i$ 对所有 $x \in \mathcal{B}(c, r)$ 和所有 i 均成立时，该包含关系成立；也就是说，当且仅当

Next, consider the containment $\mathcal{B}(c, r) \subseteq \mathcal{H}$. This holds if and only if $\|a_i\|_2 \le b_i$ holds for all $x \in \mathcal{B}(c, r)$ and all i; that is, if and only if

$$\max_{\|u\|_2 \le 1} a_i^T (c + ru) \le b_i, \quad i = 1, \dots, m$$

由于根据三角不等式

Since by the triangle inequality

$$a_i^T (c + ru) \le a_i^T c + \|a_i\|_2 \|ru\|_2$$

当 u 与 a_i 平行时等号成立，因此 $\mathcal{B}(c, r) \subseteq \mathcal{H}$ 成立当且仅当

with equality holding when u is parallel to a_i, we have that $\mathcal{B}(c, r) \subseteq \mathcal{H}$ holds if and only if

$$a_i^T c + r\|a_i\|_2 \le b_i, \quad i = 1, \dots, m$$

因此我们得到如下结论

This leads to the following

命题 4.1 球 $\mathcal{B}(c, r) \subseteq \mathcal{X}$ 可通过求解以下凸二阶锥规划来计算

Proposition 4.1 *A ball $\mathcal{B}(c, r) \subseteq \mathcal{X}$ can be computed by solving the following convex SOC program*

$$\max_{c, r, \alpha_0, \alpha_1} \quad r$$

$$\text{s.t.} \quad a_i^T c + \|A_i c - b_i\|_2 + \|r a_i + r A_i^T (A_i c - b_i)/\|A_i c - b_i\|_2 - \alpha_1\|_2 \le \alpha_0, \quad i = 1, \dots, m \tag{4.6}$$

4.2. 计算内接椭球 $\mathcal{E}$ 的方法如以上。Generalizing the approach described in the previous section, we next discuss how to compute a large (in the sense of the sum of semi-axes lengths) ellipsoid $\mathcal{E}$ inscribed in $\mathcal{X}$. We describe the ellipsoid by

[redacted]

其中，$W \in \mathbb{S}^n$ 是一个半正定矩阵（记作 W [redacted]，用于描述椭球形状；$W \in \mathbb{R}$）是椭球中心。在这种情况下，例如参见 [redacted] 中的第 10.4.3 节），若满足以下条件，则 $\mathcal{E}(c, W) \subseteq \mathcal{X}_d$ (see, e.g., Sec. 10.4.3 in [10]) that $\mathcal{E}(c, W) \subseteq \mathcal{X}_d$ if

[redacted]

对所有 u：[redacted] $\|u\|_2 \leq 1$。Posing as before, α [redacted] u and taking the maximum and minimum of the α 的最大值和最小值，我们得到等价条件：

[redacted]

当且仅当对所有 $(c, W) \subseteq \mathcal{H}_i$ 满足 [redacted] a [redacted] $\|a\|_2 \leq \sqrt{\xi_i}$ for all a $\|a\|_2 \leq 1$. Since

[redacted]

其中 [redacted] 表示 W 的谱范数（最大奇异值范数）。因此，包含关系 $\mathcal{E}(c, W) \subseteq \mathcal{H}_i$ 的一个充分（通常较保守）条件为：

[redacted]

进而可利用松弛变量 [redacted] 表示为：

[redacted]

其中 $W \succeq \gamma I$。因此我们有如下：

Proposition 4.2. *An ellipsoid $\mathcal{E}(c, W) \subseteq \mathcal{X}$ can be computed by solving the following convex SDP problem:*

[redacted]

5. Outer bounding 前几节介绍的方法旨在求出 W 的内近似。接下来，我们介绍两种旨在求出 W 外包集合的技术，从而也能求出 $\mathcal{V}$ 的外包集合。第5.1节介绍的第一种方法着重于沿给定的一组方向求出包含区间，由此确定包含 $\mathcal{V}$ 的最小外包围盒。第5.2节介绍的第二种方法讨论如何确定 $\mathcal{V}$ 的外包椭球。

5. Outer bounding. The first one in Section 5.1 focuses on finding intervals of containment along a given set of directions, which results in determination of a minimal outer box containing $\mathcal{X}$. The second technique in Section 5.2 discusses how to determine an outer-bounndig ellipsoid for $\mathcal{X}$.

[redacted]

5.1. 计算外包含盒。假设给定一个正定矩阵 W 和一个椭球 $\mathcal{X}$，满足 $\mathcal{X} = \{x \mid x^\top W x \le 1\}$，我们希望计算一个盒子 $\mathcal{X}_{\text{outer}} = \{x \mid \ell \le x \le u\}$，其中 $\ell, u \in \mathbb{R}^n$ 的选择使得 $\mathcal{X} \subseteq \mathcal{X}_{\text{outer}}$ 且 $\mathcal{X}_{\text{outer}}$ 尽可能小。

5.1. Computing an outer bounding box. Given a positive definite matrix W and an ellipsoid $\mathcal{X}$ of the form $\mathcal{X} = \{x \mid x^\top W x \le 1\}$, we seek a box $\mathcal{X}_{\text{outer}} = \{x \mid \ell \le x \le u\}$, with $\ell, u \in \mathbb{R}^n$, such that $\mathcal{X} \subseteq \mathcal{X}_{\text{outer}}$ and $\mathcal{X}_{\text{outer}}$ is as small as possible.

我们通过求解二阶锥规划，计算 $\mathcal{X}$ 沿方向 $v^{(i)}$ 的最大和最小分量

We compute the maximum and minimum components of $x \in \mathcal{X}$ along the direction $v^{(i)}$, by solving SOCPs

$$\begin{array}{ll} \max & x^\top v^{(i)} \\ \text{subject to} & x \in \mathcal{X} \end{array} \qquad \begin{array}{ll} \min & x^\top v^{(i)} \\ \text{subject to} & x \in \mathcal{X} \end{array}$$

命题 5.1. 设 $\{v^{(1)}, \ldots, v^{(n)}\}$ 是 $\mathbb{R}^n$ 中的标准正交向量集，且 $\gamma_i^{\max}$、$\gamma_i^{\min}$ 分别是通过求解 (5.1)、(5.2) 得到的、其元素为 $\min$ 和 $\max$ 的向量。那么，盒子

Proposition 5.1. Let $\{v^{(1)}, \ldots, v^{(n)}\}$ be an orthonormal basis of $\mathbb{R}^n$, and let $\gamma_i^{\min}$, $\gamma_i^{\max}$ be the vectors with entries $\gamma_i^{\min}$, $\gamma_i^{\max}$ respectively, computed by solving (5.1), (5.2). Then, the box

$$\mathcal{X}_{\text{outer}} = \left\{ x \in \mathbb{R}^n \;\middle|\; \sum_{i=1}^{n} \gamma_i^{\min} v^{(i)} \le x \le \sum_{i=1}^{n} \gamma_i^{\max} v^{(i)} \right\}$$

满足 $\mathcal{X} \subseteq \mathcal{X}_{\text{outer}}$。

contains $\mathcal{X}$, i.e., $\mathcal{X} \subseteq \mathcal{X}_{\text{outer}}$.

Proof. 任取 $x \in \mathcal{X}$。由于 $\{v^{(1)}, \ldots, v^{(n)}\}$ 构成 $\mathbb{R}^n$ 的标准正交基，因此存在系数 $\gamma_i \in \mathbb{R}$，使得 $x = \sum_{i=1}^{n} \gamma_i v^{(i)}$，而这些系数实际上是 x 在基向量方向上的分量，即 $\gamma_i = x^\top v^{(i)}$，$i = 1, \ldots, n$。根据 $\gamma_i^{\min}$ 的定义，所选点 x 满足问题 (5.1)、(5.2) 的约束，也就是说，x 是这些问题的可行解，尽管未必是最优解。因此，对 $i = 1, \ldots, n$，有 $\gamma_i^{\min} \le x^\top v^{(i)} \le \gamma_i^{\max}$，也就是说，对 $i = 1, \ldots, n$，有 $\gamma_i^{\min} \le \gamma_i \le \gamma_i^{\max}$，这意味着 $x \in \mathcal{X}_{\text{outer}}$，从而证明了包含关系 $\mathcal{X} \subseteq \mathcal{X}_{\text{outer}}$。 □

Proof. Take any $x \in \mathcal{X}$. Since $\{v^{(1)}, \ldots, v^{(n)}\}$ forms an orthonormal basis of $\mathbb{R}^n$, there exist coefficients $\gamma_i \in \mathbb{R}$ such that $x = \sum_{i=1}^{n} \gamma_i v^{(i)}$, and these coefficients are actually the components of x along the basis vectors, that is, $\gamma_i = x^\top v^{(i)}$, $i = 1, \ldots, n$. Now, by definition of $\gamma_i^{\min}$, the selected point x satisfies the constraints of problems (5.1), (5.2), that is, it is feasible albeit possibly not optimal for these problems. Hence, it holds that $\gamma_i^{\min} \le x^\top v^{(i)} \le \gamma_i^{\max}$, for $i = 1, \ldots, n$, that is $\gamma_i^{\min} \le \gamma_i \le \gamma_i^{\max}$, for $i = 1, \ldots, n$, which means that $x \in H_{\text{outer}}$, which proves the inclusion $\mathcal{X} \subseteq H_{\text{outer}}$. □

例如，可以将 $\{v^{(1)}, \ldots, v^{(n)}\}$ 取为 $\mathbb{R}^n$ 的标准基，此时我们得到一个超矩形（即与坐标轴对齐的盒）。另一种选择是，将 v 向量取为命题 4.2 中内接椭球 $\mathcal{E}$ 的 W 矩阵的正交特征向量集，它们描述了半轴的方向，这样我们便得到一个边与椭球轴对齐、且包含 $\mathcal{X}$、$\mathcal{E}$ 和 $\mathcal{X}_{\text{true}}$ 的最小盒。

For example, one can take $\{v^{(1)}, \ldots, v^{(n)}\}$ to be the standard coordinate basis of $\mathbb{R}^n$, in which case we obtain axis-aligned rectangles (i.e., orthotopes with faces aligned with the coordinate axes). Another choice would be to take as $v^{(i)}$'s the set of orthogonal eigenvectors of the W matrix of the inscribed ellipsoid $\mathcal{E}$ of Proposition 4.2, which describe the directions of the semiaxes; we find in this way the minimal box with sides aligned to the ellipsoid axes that contains $\mathcal{X}$, $\mathcal{E}$ and $\mathcal{X}_{\text{true}}$.

在实际应用的复杂度。定位中通常具有实际意义的情形涉及较小的 n（例如 $n = 2$ 或 $n = 3$）以及适中的锚点数量 $m \gg n$。因此，典型的 SOCP 问题 (5.1) 和 (5.2) 不需要针对大规模优化定制的求解方法，而是可以通过标准的原始-对偶内点算法有效求解，这些问题分别包含 $n + 1$ 个变量、m 个二阶锥约束，和 $2m$ 个线性不等式约束。根据 [20] 针对内点算法提出的经典自协调障碍复杂度框架，这些问题的障碍参数为 $\nu = 4m$，因此，达到 ϵ 精度所需的外迭代次数为 $O(\sqrt{\nu}\log(1/\epsilon)) = O(2\sqrt{m}\log(1/\epsilon))$。每次迭代又需要

Complexity and practical interest. The localization problems of practical interest involve small n (say, $n = 2$ or $n = 3$) and a moderate number of anchors $m \gg n$. Typical instances of SOCP problems (5.1) and (5.2), therefore, do not require solution methods tailored for large-scale optimization, and can be solved effectively by means of standard primal-dual interior-point algorithms for which self-concordant barrier complexity results are available. According to the classical self-concordant barrier complexity framework of [20] for interior-point algorithms, the barrier parameter for these problems is given by $\nu = 4m$, hence the outer-iteration count to reach ϵ-accuracy is $O(\sqrt{\nu}\log(1/\epsilon)) = O(2\sqrt{m}\log(1/\epsilon))$. Each iteration in turn requires

大约 $O(m)$ 次 [illegible] m^2 次浮点运算。因此，在实际定位应用中所关注的典型条件下，计算包围盒的计算工作量仍然适中。 $\star$

for computing the bounding box thus remains moderate, under the typical conditions of interest in practical localization applications. $\star$

5.1.1. Directional localization. 作为一种特例，我们还可以确定沿任意指定方向的定位不确定性范围的保证界。假设我们固定一个探测方向 $v \in \mathbb{R}^2$，$\|v\|_2 = 1$，并希望求出沿方向 v、x 相对于中心估计 $c \in \mathcal{X}$ 的不确定性范围。用公式表示，我们考虑 $x = c + \gamma v$，其中 c 和 v 已知，并求使 $x \in \mathcal{X}$ 成立的 γ 的最大值和最小值。这些值可以通过求解以下两个二阶锥规划精确计算：

5.1.1. Directional localization. As a variant, we can also ascertain guaranteed bounds on the localization uncertainty range along a desired direction. Suppose we fix a probing direction $v \in \mathbb{R}^2$, $\|v\|_2 = 1$, and we ask ourselves what is the range of uncertainty in x around a central estimate $c \in \mathcal{X}$, along direction v. In formulae, we consider $x = c + \gamma v$, with c and v given, and we seek for the maximum and minimum values of γ for which $x \in \mathcal{X}$. These values can be computed exactly by solving two SOCPs, as follows

$$\begin{aligned} \gamma_{\max} = \max_{\gamma,\alpha\in\mathbb{R}} \quad & \gamma \\ \text{s.t.}: \quad & \xi^- \le -2QA^\top(c+\gamma v) + Q\omega + \alpha\mathbf{1} \le \xi^+, \\ & \|c+\gamma v - a^{(i)}\|_2 \le \sqrt{\xi_i^+}, \quad i = 1,\dots,m, \end{aligned} \tag{5.3}$$

$$\begin{aligned} \gamma_{\min} = \min_{\gamma,\alpha\in\mathbb{R}} \quad & \gamma \\ \text{s.t.}: \quad & \xi^- \le -2QA^\top(c+\gamma v) + Q\omega + \alpha\mathbf{1} \le \xi^+, \\ & \|c+\gamma v - a^{(i)}\|_2 \le \sqrt{\xi_i^+}, \quad i = 1,\dots,m. \end{aligned} \tag{5.4}$$

5.2. 计算 $\mathcal{Y}$ 的外包椭球 [illegible] 描述的椭球 $\mathcal{O}(c,P)$. Consider an ellipsoid $\mathcal{O}(c,P)$ described by the equation

其中，$P \in \mathbb{S}^n_{++}$ 是描述椭球形状的正定矩阵，$c \in \mathbb{R}^n$ 是椭球中心。进一步考虑命题 3.1 中给出 $\mathbb{R}^n$ 的多面体 $\mathcal{X}_d$ 的表示：

where $P \in \mathbb{S}^n_{++}$ is a positive definite matrix describing the ellipsoid's shape, and $c \in \mathbb{R}^n$ is its center. Consider further the representation of the polyhedron $\mathcal{X}_d$ given in Proposition 3.1

其中，H 是 (2.8) 中定义的 RTM 中的超矩形，并且我们假设 4.1 的标准条件成立。因此，$\mathcal{X}_d$ 有界，即为一个多胞体 $\mathcal{X}_q$，其顶点 $v^{(1)}, \dots, v^{(q)}$，$q = 2^m$，可以表示为顶点 $v^{(i)}$，$i = 1, \dots, q$ 经线性映射后所得像 $w^{(i)}$ 的凸包。

where H is the hyperrectangle in $\mathbb{R}^m$ defined in (2.8), and we assume the standard conditions of Section 4.1 hold. Then, $\mathcal{X}_d$ is a polytope, i.e., a bounded polyhedron, and can be represented as the convex hull of the images $w^{(i)}$ of $v^{(i)}$, $i = 1, \dots, q$, through the linear map

因此，当 $\mathcal{X}_q \subseteq \mathcal{O}(c,P)$ 时，包含关系 $\mathcal{X}_d \subseteq \mathcal{O}(c,P)$ 得以满足，也就是说，若

Thus, when $\mathcal{X}_q \subseteq \mathcal{O}(c,P)$, the inclusion $\mathcal{X}_d \subseteq \mathcal{O}(c,P)$ is satisfied, that is if

对于包含关系 $\mathcal{O}_1 \subseteq \mathcal{O}_2$（其中 $\mathcal{O}_1$ 与 $\mathcal{O}_2$ 是式 (3.6) 中定义的椭球），我们使用 S-过程结论的一种标准充分条件，来计算覆盖椭球交集的椭球（椭球是椭球的特殊情况），参见例如 [illegible] 中的第 3 章或 [illegible] 中的第 3.2 节。以下命题成立。

For inclusion $\mathcal{O}_1 \subseteq \mathcal{O}_2$ where $\mathcal{O}_1$ and $\mathcal{O}_2$ are ellipsoids of the form (3.6), we use a standard sufficient condition resulting from the $\mathcal{S}$-procedure (which is also necessary in the case of ellipsoids) given by the $\mathcal{S}$-procedure, see, e.g., Chapter 3 of [8] or Section 3.2 in [25]. The following proposition holds.

命题 5.2（通过求解半定优化问题（半定规划）(SDP)，可以找到一个（次优的）最小体积椭球 $\mathcal{O}(c, P) \supseteq \mathcal{X}$，其中 $P \in \mathcal{S}^n_{++}$ 且 $\tau \in \mathbb{R}^m$。）

Proposition 5.2 (Outer ellipsoidal bounding via SDP): A (suboptimal) minimum-volume ellipsoid $\mathcal{O}(c, P) \supseteq \mathcal{X}$, with $P \in \mathcal{S}^n_{++}$ and $\tau \in \mathbb{R}^m$ the semidefinite optimization problem (SDP)

$$\min_{(\cdot)} \quad \log\det(\cdot)^{-1}$$

$$\text{s.t.} \quad \begin{bmatrix} 1 & (w_i - c)^\top \\ (w_i - c) & \end{bmatrix} \succeq 0, \quad i = 1, \ldots, 2^m,$$

$$\begin{bmatrix} \sum_{i=1}^{m} & \\ & \end{bmatrix} \succeq \sum_{i=1}^{2^m} \quad \begin{bmatrix} & \\ & I_n \end{bmatrix}$$

证明：第一组条件由 (5.6) 通过舒尔补得到，并蕴含 $\mathcal{O} \supseteq \mathcal{X}_v$（第 6 个线性矩阵不等式条件是将 S-过程应用于蕴含关系后得到的。

Proof: The first set of conditions, obtained from (5.6) via Schur complement, is the second linear matrix inequality condition derives from application of the $\mathcal{S}$-procedure to the implication

$$(x - 2a)^\top x \quad \|x - a\|_2^2 \quad \|x - a_i\|_2^2 \quad (x - a)(x - a)^\top \preceq$$

采用第 11.4.2.5 节中详述的方法，第二个线性矩阵不等式蕴含 $\mathcal{O} \supseteq \mathcal{H}$，因此问题 (5.7) 中的条件共同保证 $\mathcal{O} \supseteq \mathcal{X}_v \cap \mathcal{H} = \mathcal{X}$。 □

with the approach detailed in Section 11.4.2.5, the second linear matrix inequality condition implies $\mathcal{O} \supseteq \mathcal{H}$, and therefore conditions in problem (5.7) jointly enforce $\mathcal{O} \supseteq \mathcal{X}_d \cap \mathcal{H} = \mathcal{X}$. □

备注 6（椭球外包的复杂度）问题 (5.7) 是一个标准的凸半定规划，可通过原始-对偶内点法求得全局最优解。该问题包含 $2m$ 个大小为 $(n+1) \times (n+1)$ 的线性矩阵不等式块，以及一个大小为 $(2n+1) \times (2n+1)$ 的线性矩阵不等式块。根据 [20] 的经典自协调障碍框架，达到 ϵ 精度所需的外迭代次数为 $O(\sqrt{\nu}\log(1/\epsilon))$，其中 $\nu = q(n+1) + (2n+1)$，因此外迭代次数的规模为

Remark 6 (Complexity of ellipsoidal outer bounding): Problem (5.7) is a standard convex semidefinite program, can be solved to global optimality via primal-dual interior-point methods. The problem involves $2m$ LMI blocks of size $(n+1) \times (n+1)$ and one LMI block of size $(2n+1) \times (2n+1)$. According to the classical self-concordant barrier framework of [20], the outer-iteration count to reach ϵ-accuracy is $O(\sqrt{\nu}\log(1/\epsilon))$, where $\nu = q(n+1) + (2n+1)$, whence the number of outer iterations scales as

$$\mathcal{O}\left(\sqrt{q(n+1) + (2n+1)}\,\log(\cdot)\right)$$

而每次迭代本质上需要 $O(q(n+1)^2(2n+1)^3)$ 次浮点运算。因此，计算成本随 q 线性增长，并随线性矩阵不等式块的大小呈立方增长。然而，由于对 q 和 n 的依赖是指数级的，计算椭球外界比计算盒形外界更加耗费资源（参见注 5 中的复杂度分析），并且当测量值数量 m 增加时，可能变得不切实际。

while each iteration essentially requires $O(q(n+1)^2(2n+1)^3)$ floating point operations. Therefore, the computational cost grows linearly in q and cubically in the dimension of the linear matrix inequality blocks, but the dependence on n is exponential, so computing outer ellipsoidal bounds is more demanding than the computation of a box outer bound (cfr. the complexity analysis in Remark 5), and may become impractical when the number m of measurements increases. ⋆

备注 7（中心位置估计）我们可以使用命题 4.2 中计算得到的内接椭球中心 c_e，或命题 4.1 中计算得到的内接球中心 c_s 作为中心位置估计。此外，我们也可以通过外包集合获得中心估计，例如，使用命题 5.1 中给出的外包盒 $\mathcal{O}_{\text{outer}}$ 的中心，或命题 5.2 中给出的外包椭球 $\mathcal{O}$ 的中心。根据构造，内接集合的中心 c_e 和 c_s 属于 $\mathcal{X}$，但通常无法保证它们属于 $\mathcal{X}_{\text{true}}$。

*Remark 7 (Central location estimate): We can use the center c_e of the inscribed ellipsoid computed in Proposition 4.2, or the center c_s of the inscribed ball computed in Proposition 4.1 as a central location estimate. Also, we can obtain central estimates via the outer-bounding sets, e.g., via the center of the outer-bounding box H_{outer} given in Proposition 5.1, or via the center of the outer-bounding ellipsoid $\mathcal{O}$ given in Proposition 5.2. The centers c_e and c_s of the inscribed sets belong to $\mathcal{X}$ by construction, although they are in general *not* guaranteed to belong to $\mathcal{X}_{\text{true}}$.* ⋆

5.3 **算法概要：定位过程的实现。**为便于理解和实现，我们在此概述如何根据原始测量值获得集合成员外包定位估计所需的主要计算步骤。

5.3 **Algorithmic summary of the localization procedure.** For clarity and ease of implementation, we summarize here the main computational steps required to obtain the set-membership outer-bounding localization estimates from the raw measurements.

1. 输入数据：收集锚点位置 $A = [a_1 \; \cdots \; a_m]$ 以及 m 个距离测量值 $\{y_i^{(j)}\}_{j=1}^{q}$（例如，range 或 2）。根据假定的绝对误差或相对误差模型设置测量界限 $\underline{\ell}, \bar{\ell}$（参见第 2 节）。

1. Input data: Collect anchor positions $A = [a_1 \; \cdots \; a_m]$ and the m distance measurements $\{y_i^{(j)}\}_{j=1}^{q}$ (e.g., range or 2). Set the measurement bounds $\underline{\ell}, \bar{\ell}$ according to the assumed absolute or relative error model (see Section 2).

2. **Preprocessing & Outlier Check (Optional):** 解二阶锥规划 (6.6), 以求得最小界限扩大量 w, 更新 $c_+ \leftarrow c_+ + w$ 和 $c_- \leftarrow c_- - w$. 检查 $\mathcal{X}_{\text{true}}$ 是否仍在新盒内。
3. **Construct constants:** Compute matrix E (the incidence matrix of the difference-of-measurements graph, Section 3.1), vector ω, and projector $Q = (mI_m - \mathbf{1}_m \mathbf{1}_m^T)$.
4. **Outer Bounding (Box):** Choose n orthogonal directions $v^{(i)}$ (e.g., the standard basis). For each direction, solve the SOCPs (5.1) and (5.2) to find the bounds $\gamma_i^{\max}$ and $\gamma_i^{\min}$. The Cartesian product of these intervals yields the guaranteed outer bounding box H_{outer} (Proposition 5.1).
5. **Inner Approximation (Ellipsoid):** Solve the SDP (4.10) to find the maximal inscribed ellipsoid $\mathcal{E}(c, W)$ (Proposition 4.2), using the pre-computed bounds and matrices.

6. **Numerical Insights and Results:** 讨论数值结果，特别是 [specific topic]，并提供 [specific insights]。

6. Numerical insights and results

In this section we discuss some numerical issues, and we provide some additional techniques, with respect to those described in Section 5, that can be employed in practice. In particular we discuss how to deal with situations in which the measurement errors violate the assumed upper or lower bounds.

6.1. Searching locally for a feasible point

In Remark 4.1 we observed that the center of the inscribed ellipsoid $\mathcal{E} \subseteq \mathcal{X}_{\text{true}}$ may fail to belong to $\mathcal{X}_{\text{true}}$, and the same can happen for any other of the central estimates discussed in the previous sections, such as the center c_o of the outer bounding box H_{outer}. In practice, this should not be an issue, since we are mostly interested in locating X_{true} via bounding sets, hence the center of such sets still carries the key information about where approximately X_{true} is located. However, if one insists in trying to find a point which truly belongs to X_{true}, the following *local* approach can be followed.

We denote with c the central estimate we have computed, which can be the center of the outer bounding box, or the center of the inscribed ellipsoid, or other. For instance we may take c to be the center of the outer bounding box, $c = c_o$. If $c \in \mathcal{X}_{\text{true}}$ (this condition is easy to check numerically), then there is nothing else to do. If instead $c \notin \mathcal{X}_{\text{true}}$, we search locally for a possible point that belongs to $\mathcal{X}_{\text{true}}$. The key observation is that when dealing with the original nonlinear constraints (2.9) the right hand side inequality poses no problem from a computational point of view, since it represents a convex constraint on x. Contrary, the left-hand side inequality is nonconvex in x. The idea we propose is that once a neighborhood of X_{true}, and a corresponding center c, has been determined, we can approximate locally the nonconvex constraint $\|x - a^{(i)}\|_2^2 \geq \xi_i^-$ by means of its first-order approximation around point

$$[\text{illegible}]$$

that is, by using a linear inequality of the form

$$[\text{illegible}]$$

Figure 1 illustrates this idea on a simple two-dimensional example. Intuitively, this approximation works best in a neighborhood of c, which is why we search for points close to c. One approach is thus to compute a new point x that belongs to the intersection of $\mathcal{X}$ and the regions where (6.1) hold for $i = 1, \ldots, m$. In practice, since the constraints (6.1)

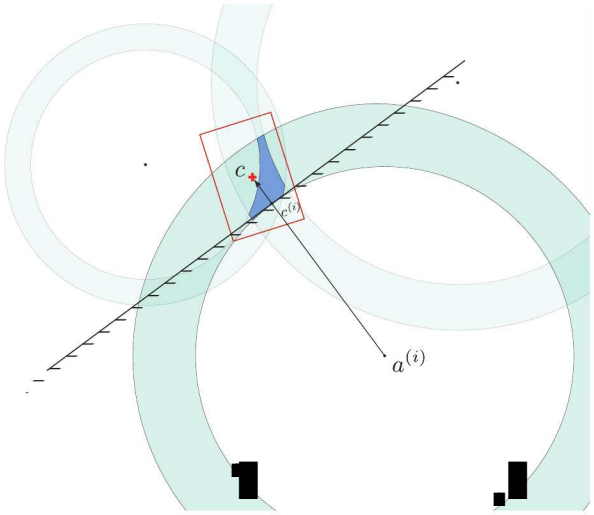

图4. 非凸约束 $\|a^{(i)} - x\|_2 \geq \xi_i$ 的局部线性近似，红色方框表示 $\mathcal{X}_{\text{true}}$，$a^{(i)}$ 其圆心为 $c^{(i)}$。在本图示中，c 不属于 $\mathcal{X}_{\text{true}}$（较深的阴影区域）。

Figure 4. Local linear approximation of the nonconvex constraint $\|a^{(i)} - x\|_2 \geq \xi_i$. The red box represents $\mathcal{X}_{\text{true}}$, with center c which, in this illustration, does not belong to $\mathcal{X}_{\text{true}}$ (the darker shaded area).

在局部比原始的约束更严格，为避免不可行性，我们添加松弛变量 s_i，以允许一定程度的违反，并在目标函数中对这类违反进行惩罚。总的来说，我们求解如下形式的凸优化问题

at the cost of violating the original constraint. To avoid infeasibility, we add slack variables $s_i \geq 0$ to allow some violation, and penalize such violations in the objective. Overall, we solve a convex optimization problem of the form

$$\begin{aligned} \text{minimize} \quad & f_0(x) + \gamma \sum_{i=1}^{m} s_i \\ \text{subject to} \quad & x \in \mathcal{X}_d, \\ & \|c^{(i)} - a^{(i)}\|_2^2 \leq \xi_i^+ \quad i = 1, \ldots, m, \\ & 2(c^{(i)} - a^{(i)})^\top (x - c^{(i)}) + s_i \geq 0, \quad i = 1, \ldots, m. \end{aligned}$$

这个问题是一个凸二次规划问题（QP），可以通过全局方法高效求解，然而（如前所指出的），线性化约束仍然只是实际非线性约束的近似，因此我们根据 (6.2) 得到的最优解 $\hat{x}$ 仍可能不属于 $\mathcal{X}_{\text{true}}$。

This problem is a convex quadratic program (QP), and can be solved efficiently by global methods. However (as already indicated), the linearized constraints are still only an approximation of the actual nonlinear constraints, whence the optimal solution $\hat{x}$ that we obtain from (6.2) may still fail to belong to $\mathcal{X}_{\text{true}}$.

6.2. 违反其假设的误差 (Errors that violate their assumed bounds)

如果 (2.2) 中的误差 e_i 超过其假定界限，相应的 ξ_i 参数超过界限 ξ_i^+ 或 ξ_i^- 之内，并且集合 $\mathcal{X}_{\text{true}}$ 非空。相反，当某些实际误差恰好超出其假定界限时，(2.9) 中的集合 $\mathcal{S}_i$ 可能没有交集，因此 $\mathcal{X}_{\text{true}}$、$\mathcal{X}_d$ 和 $\mathcal{X}$ 可能为空。在这种情况下，前几节讨论的所有凸优化问题都可能变得不可行。

If the measurement errors in (2.1) violate their assumed bounds, i.e., if the errors e_i in (2.2) happen to exceed the bounds ξ_i^+ or ξ_i^- in that ξ_i parameters are within the bounds $\xi_i^- \xi_i^+$, and the set $\mathcal{X}_{\text{true}}$ is nonempty. Contrary, when some of the actual errors happen to be outside their assumed bounds, the sets $\mathcal{S}_i$ in (2.9) may have empty intersection, hence $\mathcal{X}_{\text{true}}$, $\mathcal{X}_d$ and $\mathcal{X}$ may be empty. In such case, all the convex optimization problems discussed in the previous sections may turn out to be infeasible.

不过，可以对这些方法进行修改，以适应实际情况：某些测量值可能受到离群值影响，或者一般而言，受到不符合假定界限的误差影响。其思路很简单，就是允许扩大界限，也就是说，我们考虑可变界限 $\xi_i - \nu_i^-, \xi_i^+ + \nu_i^+$，其中 $\nu_i^+, \nu_i^- \geq 0$ 分别表示上界和下界扩大量，并且

*One described approach, however, can be modified to accommodate the practical situation in which some measurements may be affected by outliers or, in general, by errors that do not respect the assumed bounds. The idea is simply to allow for an enlargement of the bounds ξ^-, ξ^+. That is, we consider *variable* bounds $\xi^- - \nu^-, \xi^+ + \nu^+$, where $\nu^+, \nu^- \geq 0$ contain the upper and lower bound enlargements, respectively, and*

我们寻找能够保证给定半径 r 的球包含在新的、扩大的定位集 $\mathcal{X}'$ 中的最小的
我们寻找能够保证给定半径 r 的球包含在新的、扩大的定位集 $\mathcal{X}'$ 中的最小的
$r \geq 0$ is contained in the new, enlarged localization set $\mathcal{X}'$. By looking at the deri-
大量。根据第4.1节中的推导可知，若满足以下条件，球 B(c,r) 就包含在 % 中：
vations in Section 4.1 we see that a ball $B(c, r)$ is contained in $\mathcal{X}'$ if

[redacted]

对 [redacted] 成立，，且，and

[redacted]

对 [redacted] 成立，，其中后一个不等式由对(4.5)两边平方得到。给定足够小的 r，我们For
求解以下凸规划
given and sufficiently small $r \geq 0$ we solve the convex program

[redacted]

(6.6)

[redacted]

问题始终可行is 若最优解满足 [redacted]，则原定位集 $\mathcal{X}$ 非空。若最优解满足 [redacted]
$\mathcal{X}$ 或 [redacted] 为空，则 $\mathcal{X}$ 为空；但我们可以扩大误差界 [redacted] 使 [redacted]，
并保证相应的更新集 $\mathcal{X}'$ 非空且包含一个半径为 r 的球。因此，具有正值的向量 [redacted]
或 vt 表明，由于某些测量值不满足其假定界限，定位集为空。发生这种情况时，我们可以检
查 [redacted] 中正元素的大小相对于 [redacted] 中对应基准值的情况，并决定是舍弃这次实验、重
新测量，还是使用扩大的更新界限。通过标准方法继续进行位置估计。因此，问题 (6.6) 可
以在实际定位之前作为预处理步骤来求解，用于验证假定误差界的可行性、剔除离群值，或
调整误差界，使测量方程组联合可行。
and decide whether we want to discard this experiment and repeat it with new measurements, or if we want to proceed to location estimation via the standard approach applied using the updated enlarged bounds. Problem (6.6) can thus be solved as a pre-processing step, before running the actual localization, for validating the feasibility of the assumed error bounds, for removing outliers, or for adjusting the error bounds so that the measurement equations become jointly feasible.

7. 数值实验 Numerical experiments

在这些数值实验中，我们考虑带有相对加性误差 [redacted] 的测量模型 (2.2)，并对所有 7 取 [redacted]，相应的 [redacted] 以及相对界限由
In these numerical experiments, we consider the measurement model (2.2) with relative additive errors [redacted], and we take
(2.7) 给出。我们针对空间维数 [redacted] 和 [redacted] 进行实验。对于给定的 [redacted]，我们选取
$\tilde{e}_i = \tilde{e}_i^+ < 0$ for all i; the corresponding $\mathcal{E}_i$s and the relative bounds are given by (2.7). We experiment with space dimension $n = 2$ and $n = 3$. For given n, we select
整数 [redacted]，并将 m 个锚点位置 [redacted] 均匀随机地分配在 [redacted] 中，真实目标位置 [redacted] 被均匀随机地放置在 [redacted] 中，随后
integer $m \in \{n+1, \ldots, 10\}$ and assign the m anchor positions $a^{(i)}$, $i = 1, \ldots, m$, uniformly at random in $[-100, 100]^n$, and then x_{true} is placed uniformly at random in $[-100, 100]^n$. 生成 m 个含噪测量值 [redacted]，其形式为 [redacted]，其中 [redacted]
uniformly at random in $[-e_i, e_i]$.
在 [redacted] 中均匀随机生成。

对于每个随机问题实例，我们根据命题 4.2 计算内接椭球 [redacted]，并根据命题
For each random problem instance, we compute the inscribed ellipsoid $\mathcal{E}(c, P)$ according to Proposition 4.2 and the bounding box $\supset H$ according to Proposition 5.1,
5.1 计算包围盒 Hoyter，其边与椭球 [redacted] 的轴对齐。随后，我们检查 Houter 的中心
with sides aligned to the ellipsoid $\mathcal{E}$'s axes. We then check if the center c_H of H_{outer} is
cy 是否位于 Virue 中：若是，则返回 # [redacted] cy 作为中心估计；若否，则求解问题
in $\mathcal{X}_{\text{true}}$; in the positive case we return as central estimate $\hat{x} = c_h$ and in the negative case we solve problem (6.2) and return the corresponding optimal solution as estimate
(6.2)，并将相应的最优解作为估计值 & 返回。我们进一步计算 [redacted] 与真实目标位置 “
$\hat{x}$. We then evaluate, as before, the absolute position estimation error, $\|x_{\text{true}} - \hat{x}\|_2$, which represents the absolute position estimation error, and also evaluate the relative error by dividing $\|x_{\text{true}} - \hat{x}\|_2$ by the average distance of $\hat{x}$ from the anchors. Finally,
之间的实际距离，该距离表示绝对位置估计误差；同时，将 [redacted]
除以 # 到锚点的平均距离，以计算相对误差。最后，

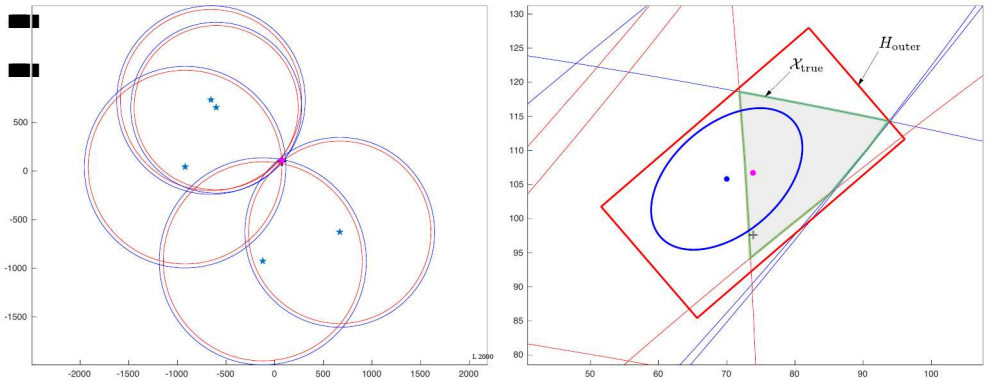

图 5: 左：锚点及其环带的交集 $\mathcal{X}_{\text{true}}$ 的外包盒（红色）以及 $\mathcal{X}_{\text{true}}$ 的内椭球近似（蓝色）。右：交集区域的放大图。

Fig. 5: Left: anchors and their annuli, the intersection $\mathcal{X}_{\text{true}}$, the outer bounding box (in red) and inner ellipsoidal approximation of $\mathcal{X} \supset \mathcal{X}_{\text{true}}$ (in red) and inner ellipsoidal approximation of $\mathcal{X} \supset \mathcal{X}_{\text{true}}$ (in blue).

we denote by $\text{half}(H_{\text{outer}})$ the average of the half-side lengths of H_{outer}.

Figure 5 shows the result for one random instance of the setup described above, with $m = 20$ anchors and relative bound $\tilde{e}_i^+ = 0.02$ (i.e., 2% relative error). The left panel shows the anchors (stars) and their measurement annuli. The right panel shows a close up of the intersection region: the outer bounding box H_{outer} is depicted in red, the inner ellipsoid $\mathcal{E}$ is depicted in blue. The black cross indicates x_{true}, and the red dot indicates c_b, which in this case does belong to $\mathcal{X}_{\text{true}}$, hence $\hat{x} = c_b$.

In numerical experiments, for each $n \in \{2, 3\}$, we selected in succession $m = N, N+1, \ldots$ until the first time that the problem (P) was feasible for 10 consecutive random draws of the anchors a_i. We recorded all the experiments three times with increasing relative error bounds $\tilde{e}_i^+ = 0.02$, $\tilde{e}_i^+ = 0.1$ and $\tilde{e}_i^+ = 0.2$. The test was coded in Matlab using CVX [12] with Mosek solver [1] for SDP and SOCP, and run on a iMac 3.2 GHz Intel Xeon desktop computer, without any particular care devoted to code optimization.

For each run we evaluated the absolute error $e(c_b) = \|c_b - x_{\text{true}}\|_2$ with respect to the box center c_b, the absolute error $e(\hat{x}) = \|\hat{x} - x_{\text{true}}\|_2$ with respect to the ball center $\hat{x}$, and the relative error $\text{ey}(\hat{x}) = e(\hat{x})/\|x_{\text{true}}\|_2$. We also recorded the average distance $\text{ey}(c_b)$ of the box center c_b from $\mathcal{X}_{\text{true}}$, and the average distance ey_{outer} of the box vertices from $\mathcal{X}_{\text{true}}$. Finally, we recorded the average $\text{half}(H_{\text{outer}})$ of the half-side lengths of the bounding box H_{outer}, and the average $\text{half}(H_{\text{inner}})$ of the half-side lengths of the inscribed ellipsoid $\mathcal{E}$. Additionally, we recorded the average $\text{vol}(H_{\text{outer}})$ of the volume of the bounding box H_{outer}, and the average $\text{vol}(\mathcal{E})$ of the volume of the inscribed ellipsoid $\mathcal{E}$. Here, $\text{vol}(\mathcal{X}) = \int_{\mathcal{X}} 1 \, dx$ denotes the volume of a set $\mathcal{X}$, and is computed via the standard formula for the volume of an ellipsoid, and as a sum of volumes of boxes for the bounding box. We also recorded the average $\text{vol}(\mathcal{X}_{\text{true}})$ of the volume of $\mathcal{X}_{\text{true}}$, which we estimated by Monte-Carlo integration, using $N_x = 10^4$ uniform random points in H_{outer}. Since $I_{\mathcal{X}_{\text{true}}}(c_b)$ corresponds to the frequency $f_{\%}(c_b)$ with which $c_b \in \mathcal{X}_{\text{true}}$, the average of $I_{\mathcal{X}_{\text{true}}}(\hat{x})$ corresponds to the frequency $f_{\%}(\hat{x})$ with which $\hat{x} \in \mathcal{X}_{\text{true}}$. Further, we evaluated the runtime t_r (in second) needed for computing the bounding box, and we assessed the conservativeness of the inclusion $\mathcal{X} \supseteq \mathcal{X}_{\text{true}}$ by estimating via a Monte-Carlo method the ratio of volumes $\eta_{\text{vol}} = \text{vol}(\mathcal{X})/\text{vol}(\mathcal{X}_{\text{true}})$, obtained by generating $N_x = 10^4$ uniform random points in $\mathcal{X}$ and counting how many of them actually fall in $\mathcal{X}_{\text{true}}$; calling N_t this number, the Monte-Carlo estimate of η_{vol} is simply N_x/N_t.

The results for $n = 2$ and $n = 3$ are reported in Table 1 and Table 2, respectively, for the relative error level $\tilde{e}_i^+ = 0.02$. The experiments were then repeated for higher error

水平 $\tilde{e}_i^+ = 0.1$ 相应结果报告于表3和表4，并进一步针对 $\tilde{e}_i^+ = 0.2$ 相应结果报告于表5和表6。

level $\tilde{e}_i^+ = 0.1$, and further for $\tilde{e}_i^+ = 0.2$, with corresponding results reported in Table 5 and Table 6.

m	$\bar{e}(c_b)$	$\bar{e}(\hat{x})$	$e_{\%}(c_b)$	$e_{\%}(\hat{x})$	δ_{outer}	$\delta_{\text{outer}\%}$	$f_{\%}(c_b)$	$f_{\%}(\hat{x})$	t_r	$\bar{t}_{\text{tot}}$
2	21.38	20.16	2.45	3.25	1.48	49.80	49	80	0.66	2.09
3	17.04	16.89	1.89	1.89	1.41	48.63	89	83	0.82	1.80
4	14.20	14.20	1.85	1.85	1.41	48.85	96	85	0.89	1.81
5	12.18	12.14	1.89	1.81	1.47	48.84	94	80	0.88	1.81
6	10.65	10.60	1.87	1.74	1.49	48.92	92	80	0.92	1.83
7	9.471	9.461	1.81	1.64	1.49	48.94	92	85	0.97	1.83
8	8.526	8.517	1.85	1.85	1.47	48.86	90	87	0.96	1.82
9	7.525	7.519	1.89	1.82	1.47	48.87	94	85	0.94	1.86

表1 在 N = 100 次随机化测试中的平均结果，TABLE 1 且相对误差水平 ey = 0.02。

Average results over $N = 100$ randomized tests, for $n = 2$ and relative error level $\tilde{e}_i^+ = 0.02$.

m	$\bar{e}(c_b)$	$\bar{e}(\hat{x})$	$e_{\%}(c_b)$	$e_{\%}(\hat{x})$	δ_{outer}	$\delta_{\text{outer}\%}$	$f_{\%}(c_b)$	$f_{\%}(\hat{x})$	t_r	$\bar{t}_{\text{tot}}$
3	10.15	10.14	1.87	1.85	1.42	48.89	86	87	0.83	1.85
4	8.508	8.504	1.80	1.89	1.43	48.85	88	84	0.82	1.86
5	7.301	7.296	1.80	1.84	1.41	48.85	89	88	0.86	1.81
6	6.339	6.330	1.82	1.85	1.43	48.84	88	85	0.86	1.89
7	5.567	5.565	1.81	1.85	1.41	48.82	90	86	0.91	1.83
8	4.935	4.927	1.80	1.81	1.41	48.89	93	82	0.89	1.86
9	4.416	4.407	1.82	1.83	1.42	48.85	90	87	0.88	1.89

表2 在 n = 3 和相对误差水平 ey = 0.02 下，进行 N = 100 次随机化测试的平均结果。

Average results over $N = 100$ randomized tests, for $n = 3$ and relative error level $\tilde{e}_i^+ = 0.02$.

m	$\bar{e}(c_b)$	$\bar{e}(\hat{x})$	$e_{\%}(c_b)$	$e_{\%}(\hat{x})$	δ_{outer}	$\delta_{\text{outer}\%}$	$f_{\%}(c_b)$	$f_{\%}(\hat{x})$	t_r	$\bar{t}_{\text{tot}}$
2	24.91	13.21	3.20	1.55	12.52	169.84	22.47	10.84	0.66	2.01
3	19.92	19.85	2.50	2.50	1.50	50.00	50	84	0.82	1.86
4	16.61	16.57	2.47	2.41	1.48	49.88	94	85	0.80	1.86
5	14.23	14.18	2.48	2.48	1.47	49.83	91	80	0.84	1.82
6	12.45	12.41	2.42	2.44	1.46	49.89	93	85	0.82	1.84
7	11.07	11.05	2.45	2.45	1.50	50.00	92	85	0.80	1.88
8	9.968	9.957	2.46	2.41	1.48	49.87	93	83	0.86	1.83
9	9.061	9.051	2.42	2.46	1.47	49.84	94	87	0.86	1.85

表 3 对于 n = 2 和相对误差水平 ey = 0.1，进行 N = 100 次随机化测试所得的平均结果。

Average results over $N = 100$ randomized tests, for $n = 2$ and relative error level $\tilde{e}_i^+ = 0.1$.

As expected, we observe that as the number m of anchors increases, the absolute and relative errors tend to decrease. In addition, we see that the local search step that computes $\hat{x}$ consistently improves the probability that the resulting estimate actually belongs to $\mathcal{V}$, compared to the plain outer box center c_b. However, the absolute and relative errors with $\hat{x}$ improve compared to c_b only for low values of m approximately, up to $m = 4$ for $n = 2$, and up to $m = 6$ for $n = 3$), while as m increases there seems to be no advantage in using $\hat{x}$ in place of c_b in terms of absolute or relative localization errors. The average time t_r for computing an outer box remains below 1.16s for $n = 2$ and below 1.72s for $n = 3$; it mildly grows with n and m, but it is insensitive to the noise level. We further observe that

[illegible]	[illegible]	[illegible]	[illegible]	[illegible]	[illegible]	[illegible]	[illegible]	[illegible]	[illegible]	[illegible]
[illegible]	[illegible]	[illegible]	[illegible]	[illegible]	[illegible]	[illegible]	[illegible]	[illegible]	[illegible]	[illegible]
[illegible]	[illegible]	[illegible]	[illegible]	[illegible]	[illegible]	[illegible]	[illegible]	[illegible]	[illegible]	[illegible]
[illegible]	[illegible]	[illegible]	[illegible]	[illegible]	[illegible]	[illegible]	[illegible]	[illegible]	[illegible]	[illegible]
[illegible]	[illegible]	[illegible]	[illegible]	[illegible]	[illegible]	[illegible]	[illegible]	[illegible]	[illegible]	[illegible]
[illegible]	[illegible]	[illegible]	[illegible]	[illegible]	[illegible]	[illegible]	[illegible]	[illegible]	[illegible]	[illegible]
[illegible]	[illegible]	[illegible]	[illegible]	[illegible]	[illegible]	[illegible]	[illegible]	[illegible]	[illegible]	[illegible]
[illegible]	[illegible]	[illegible]	[illegible]	[illegible]	[illegible]	[illegible]	[illegible]	[illegible]	[illegible]	[illegible]
[illegible]	[illegible]	[illegible]	[illegible]	[illegible]	[illegible]	[illegible]	[illegible]	[illegible]	[illegible]	[illegible]
[illegible]	[illegible]	[illegible]	[illegible]	[illegible]	[illegible]	[illegible]	[illegible]	[illegible]	[illegible]	[illegible]

表4 对N [illegible] 次随机化测试的平均结果，针对n[illegible] 以及相对误差水平ey [illegible].1。

TABLE 4

Average results over $N = 100$ randomized tests, for $n = 3$ and relative error level $\tilde{e}_i^+ = 0.1$.

[illegible]	[illegible]	[illegible]	[illegible]	[illegible]	[illegible]	[illegible]	[illegible]	[illegible]	[illegible]	[illegible]
[illegible]	[illegible]	[illegible]	[illegible]	[illegible]	[illegible]	[illegible]	[illegible]	[illegible]	[illegible]	[illegible]
[illegible]	[illegible]	[illegible]	[illegible]	[illegible]	[illegible]	[illegible]	[illegible]	[illegible]	[illegible]	[illegible]
[illegible]	[illegible]	[illegible]	[illegible]	[illegible]	[illegible]	[illegible]	[illegible]	[illegible]	[illegible]	[illegible]
[illegible]	[illegible]	[illegible]	[illegible]	[illegible]	[illegible]	[illegible]	[illegible]	[illegible]	[illegible]	[illegible]
[illegible]	[illegible]	[illegible]	[illegible]	[illegible]	[illegible]	[illegible]	[illegible]	[illegible]	[illegible]	[illegible]
[illegible]	[illegible]	[illegible]	[illegible]	[illegible]	[illegible]	[illegible]	[illegible]	[illegible]	[illegible]	[illegible]
[illegible]	[illegible]	[illegible]	[illegible]	[illegible]	[illegible]	[illegible]	[illegible]	[illegible]	[illegible]	[illegible]
[illegible]	[illegible]	[illegible]	[illegible]	[illegible]	[illegible]	[illegible]	[illegible]	[illegible]	[illegible]	[illegible]

表5

TABLE 5

Average results over $N = 100$ randomized tests, for $n = 2$ and relative error level $\tilde{e}_i^+ = 0.2$.

[illegible]	[illegible]	[illegible]	[illegible]	[illegible]	[illegible]	[illegible]	[illegible]	[illegible]	[illegible]	[illegible]
[illegible]	[illegible]	[illegible]	[illegible]	[illegible]	[illegible]	[illegible]	[illegible]	[illegible]	[illegible]	[illegible]
[illegible]	[illegible]	[illegible]	[illegible]	[illegible]	[illegible]	[illegible]	[illegible]	[illegible]	[illegible]	[illegible]
[illegible]	[illegible]	[illegible]	[illegible]	[illegible]	[illegible]	[illegible]	[illegible]	[illegible]	[illegible]	[illegible]
[illegible]	[illegible]	[illegible]	[illegible]	[illegible]	[illegible]	[illegible]	[illegible]	[illegible]	[illegible]	[illegible]
[illegible]	[illegible]	[illegible]	[illegible]	[illegible]	[illegible]	[illegible]	[illegible]	[illegible]	[illegible]	[illegible]
[illegible]	[illegible]	[illegible]	[illegible]	[illegible]	[illegible]	[illegible]	[illegible]	[illegible]	[illegible]	[illegible]
[illegible]	[illegible]	[illegible]	[illegible]	[illegible]	[illegible]	[illegible]	[illegible]	[illegible]	[illegible]	[illegible]
[illegible]	[illegible]	[illegible]	[illegible]	[illegible]	[illegible]	[illegible]	[illegible]	[illegible]	[illegible]	[illegible]

表6

TABLE 6

Average results over $N = 100$ randomized tests, for $n = 2$ and relative error level $\tilde{e}_i^+ = 0.2$.

也含关系true CCRV 的标[illegible]性（以蒙特卡[illegible]估计的体积比[illegible]衡量）似乎会随着测量值数量m的增加而适度提高，而受n的影响较小。

moderately increase with the number m of measurements while being little influenced by n.

最后，我们在测量值可能受到离群值影响的情形下测试了所提出的集合成员估计技术，即测量误差建模假定界限的情况。我们考虑了n [illegible] 且m ∈ {3,...,10} 的情形。我们假定噪声界限为2%，即ẽ⁺ [illegible].02，但仍真[illegible]实际测量噪声的生成方式如下：

Finally, we investigated the performance of the proposed set membership estimation technique in the situation where measurements may be affected by outliers, that is, by measurement errors that violate the assumed bounds. We considered the case of $n = 2$ and $m \in \{3, \ldots, 10\}$. We assumed 2% noise bounds, i.e., $\tilde{e}_i^+ = 0.02$, but the actual measurement noise was generated in the simulation as

$$z_{[illegible]} \begin{cases} [illegible] & [illegible] \\ [illegible] & [illegible] \end{cases}$$

其中，wu,ℓ在[illegible]中均匀随机生成。这意味着，1测量误差以0.9的概率满足所假设的2%界限，而以0.1的概率意外违反所假设的界限，其相对误差水平实际上可能大得多（误差最高可达50%）。对于每一对(n,m)，我们生成了

where $w_{u,\ell}$ are uniformly distributed random numbers in $[illegible]$. This means that measurement errors respect the 2% assumed bound with probability 0.9, while with probability 0.1 they unexpectedly violate the assumed bound and may actually have a much larger level of relative error (up to 50% error). For each pair (n, m) we generated

N [redacted] random problem instances and, for each one, we first solved problem (6.6), obtaining the optimal radius r, and then solved problem (6.5) with r = 1.01 r, i.e., with the radius increased by 1%. These solutions were then used to check whether, when the noise bounds were enlarged by the minimal amounts ε⁻ᵢ, ε⁺ᵢ that guarantee that the updated bounds ε̄⁻ᵢ = εⁱ⁻ + ε⁻ᵢ, ε̄⁺ᵢ = εⁱ⁺ + ε⁺ᵢ would correspond to a nonempty localization set X that contains a ball of radius r. After this pre-processing step, we solved normally, as in the previous experiments, for an inner ellipsoid and an outer bounding box, using the updated noise bounds computed in the pre-processing step. Notice that such pre-processing step also serves as an outlier detection method, since whenever we find that [redacted], we know that some of the measurement errors did not respect the original bounds. The results of such experiments, averaged over the 100 runs, are reported in Table 7. These results are to be compared to those in Table 1, where we had the same assumed error bounds but no outliers.

m	$e(c_b)$	$e(\hat{x})$	$e_{\text{outer}}(c_b)$	$e_{\text{outer}}(\hat{x})$	e_{outer}	$e_{\text{outer}\%}$	$f_{\%}(c_b)$	$f_{\%}(\hat{x})$	t	t_{vol}
[redacted]										

TABLE 7

Average relative error w.r.t. [redacted] for [redacted] simulations, with [redacted] vertices, and level $\bar{e}_i^+ = 0.2$ and 10% probability of relative error of 50%.

关于表7的结果，有几点需要说明。首先，我们注意到，平均运行时间t略高于表1中的时间，因为其中计入了预处理所需的额外工作，即求解问题（6.6）。其次，我们注意到，这一问题，从而使V非空。不过，界限的调整以使“勉强可行”为目标，也就是说，我们寻求能够保证一个小球包含在V中的最小界限调整。因此，即使进行了预处理，在存在违反假定界限的误差时，我们仍预期Y集合会小于表1中无离群值时得到的集合。事实上，这一点反映在表7的e_{outer}和$e_{\text{outer}\%}$列中，这些列衡量包围盒的大小，其值看起来小于表1中对应包围盒的值。存在离群值时，真实可行集V变得更小或为空，这一点也反映在寻找可行点的难度增加上（参见$f_{\%}(c_b)$和$f_{\%}(\hat{x})$列），以及701列中较高的值。表1中离群值误差导致的不确定性增加，自然也会体现为更大的估计误差（中心估计到真实目标位置的绝对距离或相对距离），如表7前四列所示。我们指出，在这些数值测试中，我们使用的模型超出了其预期适用范围，也就是说，仿真条件严重违反了模型本身的基本假设（即噪声应包含在假定界限内）。然而，即使在这种“超范围”使用情况下，我们提出的方法仍能给出一致的结果，并可用于验证或否定有关噪声界限的工作假设。

备注8（与点估计器的比较）。文献中提出了多种复杂的点估计器，用于高斯噪声假设下的定位，例如[28]中的凸优化方法，或[16]中的扩散高斯牛顿方法。虽然这类方法能够有效地最小化点估计的均方根误差（RMSE）等指标，但我们的方法从根本上将范式从点估计转向有保证的集合外包。在区间型未知但有界（UBB）噪声模型下，直接使用RMSE进行比较在概念上并不恰当：我们的首要目标是保证对于任何可容许噪声实现，真实位置都完全落在所计算的集合内；而随机点估计器并非为满足这一性质而设计。因此，尽管可以从我们的界定集中提取点估计（例如其几何中心），但将它们的RMSE与专门针对高斯噪声设计的点估计器进行比较，超出了集合成员框架的预期范围。⋆

Remark 8 (Comparison with point estimators). Various sophisticated point estimators have been proposed in the literature for Gaussian noise assessment, such as the interior point bias treatment in [16] or the diffusion Gauss Newton method in [28]. While such methods effectively minimize metrics like the Root Mean Square Error (RMSE) of the point estimate, our approach fundamentally shifts the paradigm from point estimation to *guaranteed set outer bounding*. Under an interval unknown-but-bounded (UBB) noise model, a direct comparative analysis using RMSE is conceptually misaligned. Our primary objective is to guarantee that the true location lies entirely within the computed set for *any* admissible noise realization, a property that stochastic point estimators are not designed to fulfill. Therefore, while point estimates can be extracted from our bounding sets (e.g., their geometric centers), comparing their RMSE against specialized Gaussian-noise point estimators falls outside the intended scope of the set-membership framework. ⋆

8. Conclusions. 本研究探讨了如何根据含噪但有界的距离测量值，求得物体位置的集合值估计。我们提出的方法可以计算出一个凸区域（定位集 $\mathcal{X}$），或其外包椭球），并保证该区域包含与测量值相符的所有可能位置所构成的集合 $\mathcal{X}_{\text{true}}$。一方面，这种有保证的集合隶属信息在某些应用中可能十分有用且至关重要；另一方面，它具有明确的几何意义，并且能够通过凸规划高效、直接地计算，无需采用线性化或松弛。

8. Conclusions. In this paper we have investigated how to obtain a set-valued estimate of an object's position from noisy distance measurements to known anchors. While standard location estimators only provide a single point estimate, the proposed approach returns a region (the localization set $\mathcal{X}$, or its outer bounding box or ellipsoid) which is *guaranteed* to contain the whole set $\mathcal{X}_{\text{true}}$ of the possible locations compatible with the measurements. On the one hand such guaranteed set-membership information can be useful and critical in certain applications, and on the other hand it has a clear geometrical meaning, and it can be computed efficiently and directly by means of convex programming, with no need to resort to linearizations or relaxations.

Several interesting research questions are open. For instance, it would be of interest to characterize the conditions under which $\mathcal{X}_{\text{true}}$ is a singleton, i.e., the measurements uniquely determine the object's position. Also, the inner relation between the localization set $\mathcal{X}$ and the anchors' configuration could be explored quantitatively. Also, inner approximations of $\mathcal{X}_{\text{true}}$, or even just the determination of one point in this set, remains a problem worth additional investigation, although heuristics exists for its solution, e.g., linearization methods such as the one described in Section 6.1, or sampling-based methods. Further, one may consider the case where the anchors' locations are not known exactly, and investigate the effect of such uncertainty on the localization set.

有若干值得进一步研究的问题。例如，可以形式化地探究包含关系 $\mathcal{X}_{\text{true}}$ 的限定性，即定量评估其与锚点配置几何之间的关系。此外，$\mathcal{X}_{\text{true}}$ 的内近似，乃至仅确定该集合中的一个点，仍是值得进一步研究的问题，尽管已有一些可用于求解的启发式方法，例如第6.1节所述的线性化方法，或基于采样的方法。此外，还可以考虑锚点位置并非精确已知的情形，并研究这种不确定性对定位集的影响。

参考文献 REFERENCES

[1] MOSEK ApS, *MOSEK 工具箱 for MATLAB 手册，版本 9.0*, 2019. 见 *MOSEK Optimization Toolbox for MATLAB. User's Manual. Version 9.0.*, 2019, http://docs.mosek.com/9.0/toolbox/index.html.

[2] S. BANCROFT, *An algebraic solution of the GPS equations*, IEEE Transactions on Aerospace and Electronic Systems, 21 (1985). S. BANCROFT，GPS 方程的代数解，IEEE 航空航天与电子系统汇刊，21（1985）。

[3] R. BAPAT, *Graphs and Matrices, 2nd Ed.*, Springer, 2014. R. Bapat，《图与矩阵》，第 2 版，Springer，2014。

[4] A. BECK, P. STOICA, AND J. LI, *Exact and approximate solutions of source localization problems*, IEEE Trans on Signal Processing, 56 (2008). A. Beck、P. Stoica 和 J. Li，源定位问题的精确解和近似解，IEEE《信号处理汇刊》，56（2008）。

[5] A. BEN-TAL, L. E. GHAOUI, AND A. NEMIROVSKI, *Robust Optimization*, Princeton Series in Applied Mathematics, Princeton University Press, 2009. A. Ben-Tal、L. E. Ghaoui 和 A. Nemirovski，《鲁棒优化》，应用数学普林斯顿系列，普林斯顿大学出版社，2009。

[6] A. BEN-TAL AND A. NEMIROVSKI, *Robust solutions of uncertain linear programs*, Mathematical Programming, 99 (2004), pp. 351–376, https://doi.org/10.1007/s10107-003-0454-4. A. Ben-Tal 和 A. Nemirovski，不确定线性规划的可调鲁棒解，《数学规划》，99（2004），第 351-376 页，https://doi.org/10.1007/s10107-003-0454-4。

[7] D. BERTSEKAS, *Convex Analysis and Optimization*, Athena Scientific, 2003. D. Bertsekas，《凸分析与优化》，Athena Scientific，2003。

[8] P. Biswas, T.-C. Liang, K.-C. Toh, Y. Ye 和 T.-C. Wang，*针对含噪距离测量的传感器网络定位的半定规划方法*，IEEE 自动化科学与工程汇刊，3（2006），第 360–371 页，https://doi.org/10.1109/TASE.2006.877401。

[9] S. BOYD, L. E. GHAOUI, E. FERON, AND V. BALAKRISHNAN, *Linear Matrix Inequalities in System and Control Theory*, SIAM Studies in Applied Mathematics, 1994. S. Boyd、L. E. Ghaoui、E. Feron 和 V. Balakrishnan，《系统与控制理论中的线性矩阵不等式》，SIAM 应用数学研究，第 15 卷，美国工业与应用数学学会，费城，宾夕法尼亚州，1994，https://doi.org/10.1137/1.9781611970777。

[10] P. Biswas, T.-C. Liang, K.-C. Toh, Y. Ye, T.-C. Wang, *Semidefinite programming approaches for sensor network localization with noisy distance measurements*, IEEE Transactions on Automation Science and Engineering, 3 (2006), pp. 360–371, https://doi.org/10.1109/TASE.2006.877401.

[11] G. C. CALAFIORE, L. CARLONE 和 M. WEI，*一种用于距离的分布式高斯牛顿方法*

多智能体编队控制的分布式高斯-牛顿方法，IEEE《控制论汇刊》，2010，第 1152-1157 页。https://doi.org/10.1109/CACSD.2010.5612770。P. CALAFIORE 和 L. E. GHAOUI，《优化模型》，剑桥大学出版社，英国剑桥，2014，https://doi.org/https: //doi.org/10.1017/CBO9781107279667。Y. T. CHAN 和 K. C. Ho，一种简单高效的双曲线定位估计器，IEEE《信号处理汇刊》，42（1994），M. GRANT 和 S. Boyd，CVX：用于规范凸规划的 Matlab 软件，2.1 版，https://cvxr.com/cvx，2014 年 3 月。M. HENK，J. RICHTER-GEBERT 和 G. M. ZIEGLER，凸多胞体的基本性质，载于《离散与计算几何手册》，J. E. Goodman，J. O'Rourke 和 C. D. Tóth 编，CRC Press，2017，1–1ULIN，鲁棒集合成员状态估计：在水下机器人技术中的应用，《Automatica》，45（2009），第 202-206 页。该文介绍了在实际机器人传感器应用中采用严格区间有界误差模型的代表性奠基工作。K. KHOSHELHAM 和 S. O. ELBERINK，Kinect 深度数据精度与分辨率，《Sensors》，12（2012），第 1437-1454 页。该文为常用室内测距传感器中的有限量化误差指标提供了实证表征。S. Kim，J. Kim 和 J.-H. KIM，用于优化处理与定位测量定位中偏差的算法，IEEE《车辆技术汇刊》，62（2013），第 2913-2925 页。D. Li 和 J. H. Hu，基于高能的“绑定位约束的最小二乘解，载于《移动与无线网络/高性能科学与工程计算/网络设计与架构/光网络控制与管理/自组织与传感器网络/编辑部会议》，2004，第 443-446 页，https: //doi.org/10.1109/ICPPW.2004.1328053。K. KHOSHELHAM 和 S. O. ELBERINK，*Accuracy and resolution of kinect depth data for indoor mapping applications*，Sensors，12（2012），pp. 1437–1454。Provides empirical grounding for https://doi.org/10.1016/j.automatica.2020.109032。G. NADDAFZADEH-SHIRAZI，M. B. SHENOUDA 和 L. LAMPE，针对存在锚点位置不确定性的传感器网络定位的三阶锥规划，IEEE《无线通信汇刊》，13（2014），第 749-763 页。https://doi.org/10.1109/TWC.2013.120613.130170。Y. NESTEROV 和 A. NEMIROVSKI，《内点多项式算法》，SIAM 应用数学研究丛书第 13 卷，美国工业与应用数学学会，费城，宾夕法尼亚州，1994，https://doi.org/10.1137/1.9781611970791。X. Su，G. MAO，B. ANDERSON，Z. YANG 和 J. CHE，*Robust localization using range measurements with unknown and bounded errors*，IEEE《控制论汇刊》，第 156-168 页，B. YANG，Q. QIU，Q.-L. HAN 和 F. YANG，基于接收信号强度指示的室内定位：采用分布式集合成员滤波，IEEE《控制论汇刊》，

[22] S. Thrun, W. Burgard, and D. Fox, *Probabilistic Robotics*, MIT Press, Cambridge, MA, 2005. Discusses sensor measurement models, including truncated and bounded characteristics for rangefinders.

[23] P. Tseng, *Second-order cone programming relaxation of sensor network localization*, SIAM Journal on Optimization, 18 (2007), pp. 156–185, https://doi.org/10.1137/050640308, https://doi.org/10.1137/050640308, https://arxiv.org/abs/https://doi.org/10.1137/050640308.

[24] Z. Wang, X. Shen, H. Liu, F. Meng, and Y. Zhu, *Dual set membership filter with minimizing nonlinear transformation of ellipsoid*, IEEE Transactions on Automatic Control, 66 (2021), pp. 5423–5430, https://doi.org/10.1109/TAC.2020.3046320.

[25] Z. Wang, X. Shen, and Y. Zhu, *On equivalence of major relaxation methods for minimum ellipsoid covering intersection of ellipsoids*, Automatica, 107 (2019), pp. 563–570, https://doi.org/10.1016/j.automatica.2019.06.007.

[26] Z. Wang, X. Zhang, A. Lambert, L. Shi, and W. Wang, *A set-membership approach for visible light positioning with fluctuated RSS measurements*, IPIN (Short Papers/Work-in-Progress Papers), (2019).

[27] E. Widdison and D. Long, *A review of linear multilateration techniques and applications*, IEEE Access, 12 (2024), https://doi.org/10.1109/ACCESS.2024.3361835.

[28] Y. Wu, X. Wang, and Y. Shen, *Adaptive range-based target localization using diffusion GN method*, IEEE Transactions on Signal and Information Processing over Networks, 8 (2022), pp. 156–168.

[29] B. Yang, Q. Qiu, Q.-L. Han, and F. Yang, *Received signal strength indicator-based indoor localization using distributed set-membership filtering*, IEEE Tran. on Cybernetics,

52 (2022), 第 5041–5057 页, https://doi.org/10.1109/TSP.2022.3198167。[illegible] Y. ZHANG, B. CHEN, Z. WANG, W. ZHANG, L. Yu, 和 L. Guo, 《多传感器系统的分布式区间并行多面体融合估计》, arXiv 预印本 arXiv:2502.17752 (2025)。

[31] G. Zeng, B. Mu, J. Chen, Z. Shi, and J. Wu, *Global and asymptotically efficient localization from range measurements*, IEEE Transactions on Signal Processing, 70 (2022), pp. 5041–5057, https://doi.org/10.1109/TSP.2022.3198167.

[32] Y. Zhang, B. Chen, Z. Wang, W. Zhang, L. Yu, and L. Guo, *Distributed zonotopic fusion estimation for multi-sensor systems*, arXiv preprint arXiv:2502.17752, (2025).

[illegible] W. Yu, E. ZAMorA, 和 A. Sorta, 《椭球同步定位与地图构建：一种用于同时定位与建图的新型集合成员方法》, Autonomous Robots, 40 (2016), 第 125–137 页, https://doi.org/10.1007/s10514-015-9443-2。[illegible] G. ZENG, B. MU, J. CHEN, Z. SHI, 和 J. WU, 《基于距离测量的全局且渐近高效定位》, IEEE 信号处理汇刊, 70 (2022), 第 5041–5057 页, https://doi.org/10.1109/TSP.2022.3198167。[illegible] Y. ZHANG, B. CHEN, Z. WANG, W. ZHANG, L. Yu, 和 L. Guo, 《多传感器系统的分布式区间并行多面体融合估计》, arXiv 预印本 arXiv:2502.17752 (2025)。